Schweizerische Eidgenossenschaft
Confédération suisse
Confederazione Svizzera
Confederaziun svizra

Federal Department of the Environment, Transport, Energy and Communications DETEC

**Swiss Federal Office of Energy SFOE**
Energy Research and Cleantech Division

**Final report dated** 25 March 2024

# IMPALA

# Impact of aggregated electrical assets on the power system stability

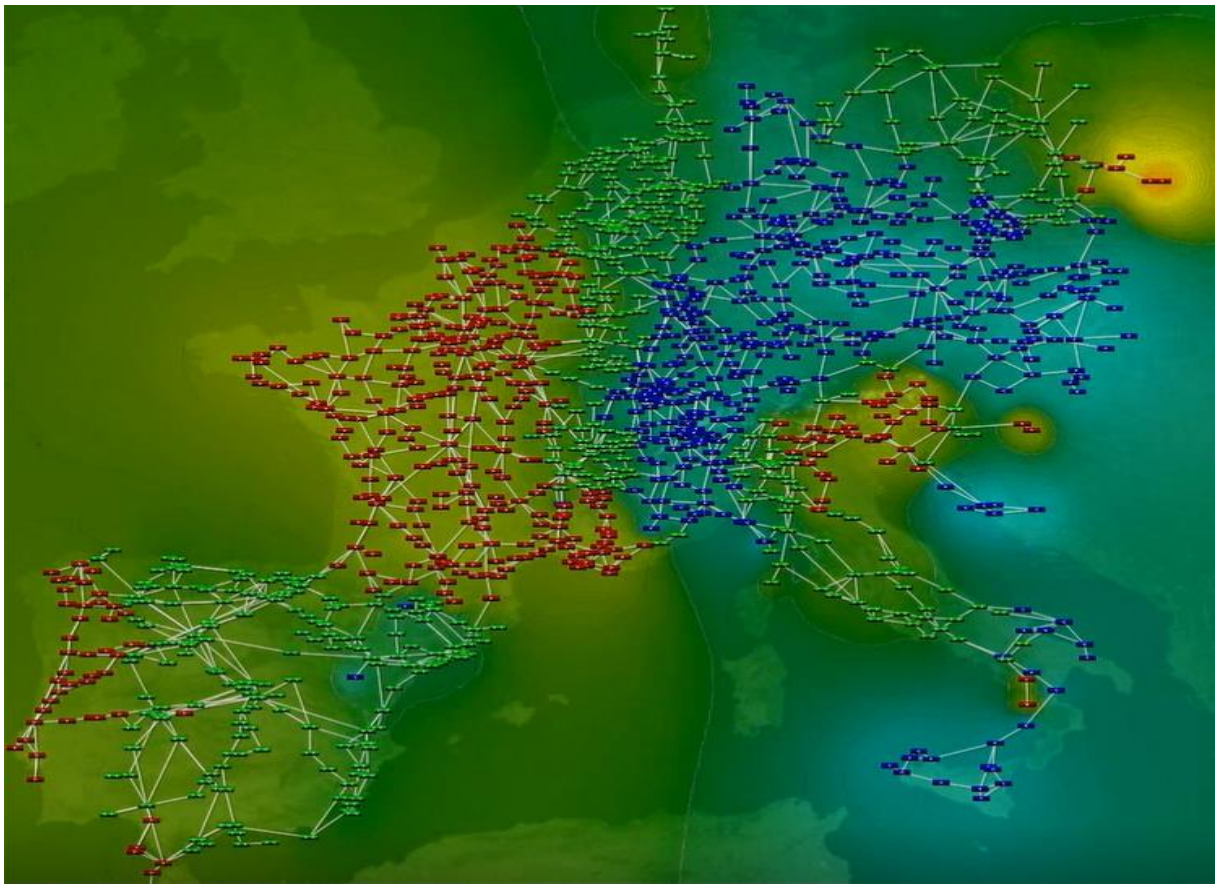

**Source:** ©2023

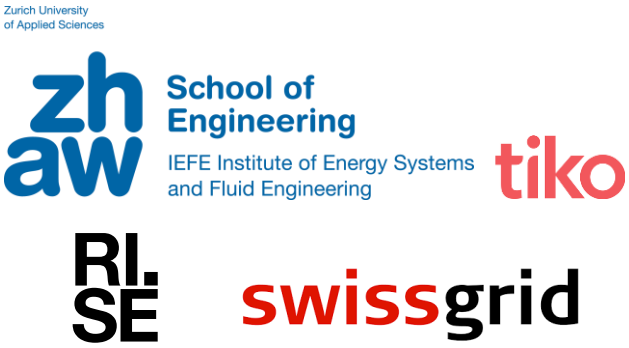


**Date:** 25 March 2024

**Location:** Bern

**Publisher:**
Swiss Federal Office of Energy SFOE
Energy Research and Cleantech
CH-3003 Bern
www.bfe.admin.ch

**Co-financing:**
tiko Energy Solutions AG
Pflanzschulstrasse 7, CH-8004 Zürich
https://tiko.energy

**Subsidy recipients:**
Zurich University of Applied Sciences (ZHAW)
Gertrudstrasse 15, CH-8401 Winterthur
www.zhaw.ch

**Authors:**
Miguel, Ramirez-Gonzalez, ZHAW, ramg@zhaw.ch
Artjoms, Obushevs, ZHAW, obus@zhaw.ch
Felix Rafael, Segundo Sevilla, ZHAW, segu@zhaw.ch
Petr, Korba, ZHAW, korb@zhaw.ch

**SFOE project coordinators:**
Dr Michael Moser, michael.moser@bfe.admin.ch

**SFOE contract number:** SI/502170-01

# Summary

Since the aggregation of resources such as distributed loads, generation, and storage can provide diverse benefits in terms of collective capacity and optimized operation, the proliferation of household assets connected to a cloud and controlled purely through an internet connection is growing more and more. However, such clouds can turn into system's hazards given that any internet-based service is prone to communication problems and susceptible to cyber-attacks. Furthermore, any outage caused by these virtual aggregated cloud grids of assets must also be compensated by the power system operator using procured control reserves. However, the amount of available power for primary reserve might be insufficient to cover a simultaneous disconnection/reconnection of the devices involved at some instant. Even though they can be intentionally controlled for balancing purposes, the non-intentional and undesired control actions may significantly affect the stability of the power system, lead to dramatic cascading effects, and result in a system collapse.

Considering the aforementioned issues, this report presents the obtained results of the research conducted to evaluate the frequency stability of the Continental European power system when subjected to the malfunction or sudden loss of large pools of original equipment manufacturer (OEM) assets. A set of key activities were carried out to accomplish the main pursued goal, including the definition of scenarios and study cases for current and future conditions of the study system, the development of the approach to represent and implement the malfunction of large asset pools and their impact on frequency dynamics, the analysis and quantification of these effects, and the lab based evaluation and testing of devices to be used in the prevention of outage spread. The future development of the system was addressed here in terms of reductions of overall system inertia (assuming potential penetrations levels of converter-interfaced generation). Non-intentional and undesired control of cloud-based assets was defined and applied in terms of the sudden and simultaneous disconnection/connection of collective power randomly accommodated across the entire system. A quantification of related impacts was performed according to the resultant transient frequency deviation and RoCoF for a set of power imbalances and variations in the equivalent inertia of the system under both interconnected operation and system split simulation cases. Furthermore, a lab-scale setup was assembled (based on a real-time power system simulator and tiko boxes) for the detection of grid separation according to frequency deviations measured with tiko hardware.

Based on extensive simulations with the Initial Dynamic Model of Continental Europe and modelling of different realistic transmission system scenarios in collaboration with the national transmission system operator (Swissgrid), the results show that RoCoFs are generally small during interconnected operation (even under low inertia scenarios). However, considered system split cases revealed RoCoFs higher than 1 Hz/s, with even more critical values under increasing system inertia reductions. Then, with the proliferation of cloud aggregated assets, events related to active power deficits exceeding the actual frequency containment reserves (FCR) of 3 GW may become more frequent and common, rising the potential risk of unacceptable frequency dynamics due to insufficient containment capability of the system.

Since system splits may expose parts of the grid to severe operating conditions, particularly in islands with insufficient generation reserve, the automatic islanding detection becomes very important to appropriately deal with the resultant isolated subsystems so that resynchronization of them and restoration of the whole system can be accomplished as fast as possible. In this sense, results related to the testing and evaluation of industrial devices (provided by tiko AG) to detect possible separation of the grid and trigger emergency control actions, such as load shedding, are also provided based on a lab-scale cyber-physical testbed and Hardware-in-the-Loop techniques.

# Main findings

- For interconnected operation, the observed RoCoF under system inertia variations and different power imbalances triggered by disconnection/reconnection of aggregated assets was relatively small. However, split scenarios showed RoCoFs larger than 1 Hz/s, with even more critical values as equivalent inertia is further reduced.
- Cloud aggregated assets raise the potential incidence of more severe active power imbalances. Therefore, a review of the FCR in CE is recommended to take into account the malfunction of large OEM asset pools.
- Based on the devices facilitated by the industrial partner, the implemented decentralized frequency regulation method to support system frequency under emergency situations showed to be a viable scheme that could be adopted in the close future (large OEM asset pools need to consider LFSMs in their pools according to TSOs requirements).

# Contents

# Abbreviations

| | |
|---|---|
| CIG | Converter-Interfaced Generation |
| EV | Electric vehicles |
| FCR | Frequency Containment Reserve |
| HIL | Hardware-in-the-Loop |
| ICT | Information and Communication Technology |
| IDMCE | Initial Dynamic Model of Continental Europe |
| ISGAN | International Smart Grids Action Network |
| LFSM | Limited Frequency Sensitive Mode |
| NRL | No Reserve Limitation |
| OEM | Original Equipment Manufacturer |
| REE-Lab | Renewable Electrical Energy Laboratory |
| RISE | Research Institute of Sweden |
| RoCoF | Rate of Change of Frequency |
| SG | Synchronous Generator |
| TSO | Transmission System Operator |
| UFLS | Under-Frequency Load Shedding |
| WPn | Work Package n |
| ZHAW | Zurich University of Applied Sciences |

# 1 Introduction

## 1.1 Background information and current situation

There are currently about 100 GW of PV power installed in the Continental European power system [1] that influences both the demand and supply sides of the electrical grid, except for the cases where they are equipped with energy storage systems, which is an unpopular configuration today for small behind-the-meter installations. In most of the cases, the solar energy is self-consumed in home appliances, which can be considered a sudden variation of the power demand for the system operators. On the other hand, surplus energy that is not self-consumed is sent back to the grid, causing potential sudden alterations of the power supply in the network. Additionally, the number of electric vehicles (EVs) connected to the grid is growing, mostly affecting the demand side's power patterns. In this sense, the 3 GW of primary reserve [2] procured across Europe corresponds to charging approximately 10 thousand EVs with fast chargers at 300 kW or charging 300 thousand EVs with domestic chargers at 10 kW. Furthermore, it is worth noticing that today, over 1 million plug-in EVs are registered in Europe, and the numbers are rising [3], [4]. Now, the same trend can be observed in pools of cloud aggregated assets, such as decentralized loads, generation, and energy storage systems, that exchange power with the grid in one or both directions. Since the aggregation of these resources can provide diverse benefits in terms of collective capacity and optimized operation [5], business models relying on the deployment of this approach through cloud and internet services are being stablished [6], with the consequent risks arising from communication failures or cyber-security breaches [7].

Considering that over 30% of all PV inverters and most charging stations are now connected to a cloud service, then the current amount of power for primary reserve would not be sufficient to cover a simultaneous disconnection/reconnection of these devices. In general, although aforementioned devices can be intentionally controlled for balancing purposes, the control of the pool through the cloud may fail or be hacked and misused by hackers. Within this context, the analysis of the effects caused by the malfunction or sudden loss of large pools of Original Equipment Manufacturer (OEM) assets, in terms of system frequency response and performance, becomes very important for the secure operation of the grid. Naturally, the related non-intentional and undesired control actions also raise the questions about grid frequency stability and the amount of power to be procured and kept available for control reserves in the future. Since the frequency stability status of a given system can be appropriately assessed from the rate of change of frequency and the transient frequency deviation, these parameters are usually monitored by TSOs to trigger protection actions. However, severe power imbalances may give place to critical rates of change of frequency, which jeopardize the effectiveness of load shedding schemes, and lead to frequency deviations that cause the trip of generating units, aggravating even more a particular condition of the system.

## 1.2 Purpose of the project

The purpose of the project is to carry out system studies and investigate time-domain simulations considering realistic scenarios to quantify the impact and negative effects to the transmission power system caused by malfunction of large OEM asset pools, which are connected via internet. In this case, the definition of malfunction represents the sudden loss of the communication channel between the asset and the service provider. Although the malfunction might be caused by hardware/software failure, cyber-attacks or information and communication technology (ICT) cloud services, investigating the nature of the communication error is beyond the context on this project. The central task to be carried out here consist of investigating the malfunction effects with respect to the stability and performance of the transmission network (in terms of frequency response).

## 1.3 Objectives

The objectives of the project are listed below:

- To model different realistic transmission system scenarios of Continental Europe using the initial dynamic model developed by ENTSO-E.
- To investigate if the present amount of ancillary services procured is enough to cover the current and future conditions of the system.
- To quantify the stability effects caused by the malfunction of large pools of assets connected via internet.
- To disseminate the results in the scientific community in the form of one or more scientific publications.
- To develop a lab-scale setup for the evaluation and testing of commercial devices that act against outage spreading.

# 2 Test system model and methodology

For the purpose of this work, a comprehensive representation of the Continental European synchronous area given by the Initial Dynamic Model of Continental Europe (IDMCE) [8] was considered. The IDMCE can approximate the overall dynamic response of the corresponding real network in terms of power system inertia, frequency containment reserve and dominant inter-area oscillations. Considering the entire ENTSO-E transmission system, the model encompasses the representation of only 26 areas, associated one to one with a particular country, as illustrated in grey color in Fig. 2.1.

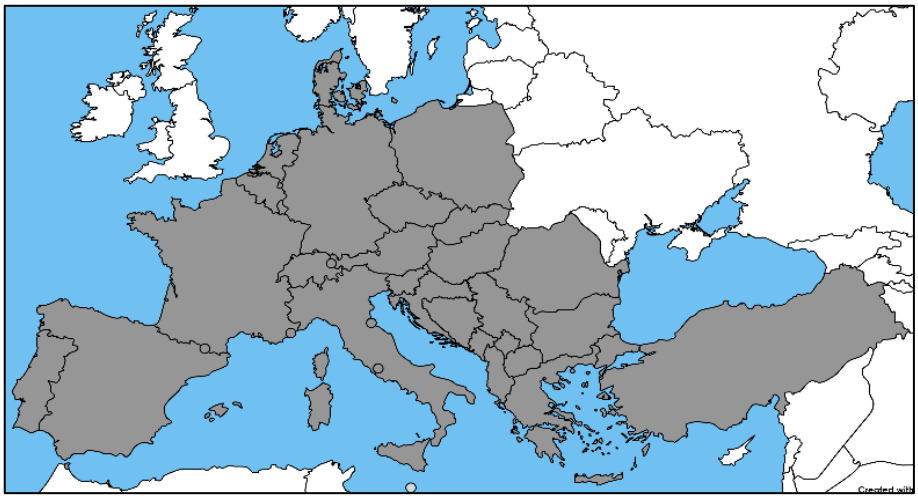

Fig. 2.1 Representative area covered by the IDMCE.

In general, the IDMCE is a very large-scale dynamic model which involves the simulation of many components such as approximately 23000 buses, 6000 generating units, 7000 loads, 18000 lines, and 9000 transformers. The model was originally configured to portray the steady state operating conditions of the real system based on a peak demand case for the year 2020 (base case scenario). According to this, the base case scenario comprises 465 GW of total generation, and 458 GW of total system load.

The events considered in the simulation studies with the IDMCE were basically system imbalances leading to frequency declines due to a shortfall of power. From this perspective, different perturbations such as generation outages, load increases, and system splits were simulated. Then, a failure or non-intentional and undesired control of cloud-based assets (due to cybersecurity issues) was emulated for example through the disconnection/reconnection of a predefined amount of collective power, which was accommodated in a decentralized way with available generators and loads across the whole system. Since active power reserves for primary frequency control are not limited in the IDMCE, some adjustments were made to the available model to limit these reserves to the reference value of 3 GW for a more realistic frequency response. Moreover, the future development of the grid regarding potential penetrations levels of renewable energy resources interfaced through power electronics converters was considered through potential scenarios of overall system inertia reduction. All the simulation studies with the IDMCE were carried out in DIgSILENT PowerFactory.

# 3 Impact of aggregated electrical assets on frequency dynamics

## 3.1 Scenarios for the current conditions of the system

From the base case scenario, different study cases were prepared and simulated to investigate the potential impact of cloud aggregate assets due to unintentional or provoked failure under current overall inertia of the system. All considered scenarios (operating points, disturbances, target powers, etc.) were determined in collaboration with the project partners (Swissgrid AG, Tiko Energy Solutions AG, and the RISE Research Institutes of Sweden) in order to be representative of realistic operating conditions of interest. Simulation results in this sense are illustrated through consequent frequency dynamics at predefined buses in Switzerland (CH), Portugal (PT), and Turkey (TR), as indicated in the map of Fig. 3.1.

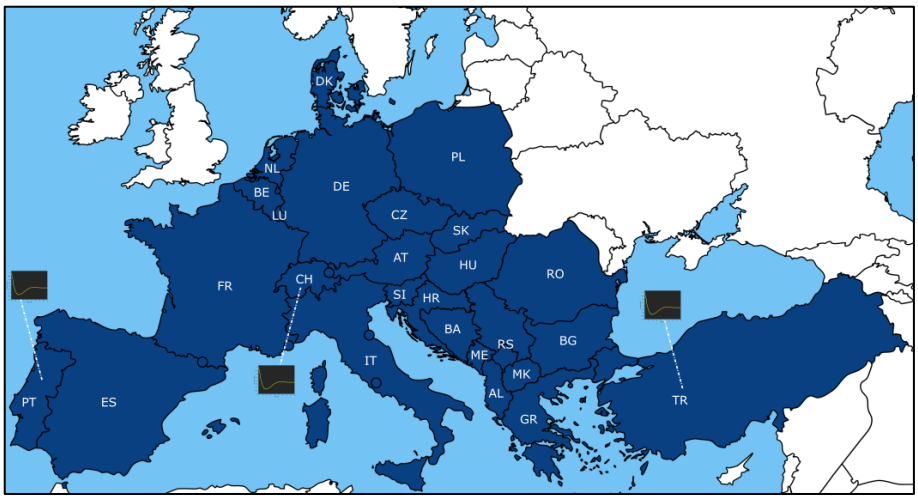


Fig. 3.1 Location of buses for monitoring of frequency dynamics.

Considered study cases and related results in terms of frequency response are provided next. It is important to highlight here that since the information contained in the IDMCE is in general anonymized, specific system components in the study cases are denoted according to the identifier given by the

simulation model. Besides, involved generators refer to single conventional generating units (as originally modelled in the IDMCE).

### 3.1.1 Case 1: Generation outage of 2.61 GW in Switzerland (CH)

For this case, generators CH_911689_1, CH_911682_1, CH_911692_1, and CH_911696_1, were selected to be simultaneously disconnected. The disturbance is applied at 1 s and the obtained response is shown in Fig. 3.2.

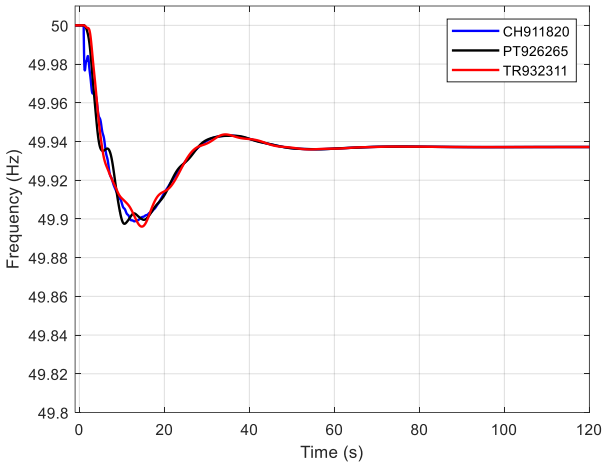


Fig. 3.2 Frequency dynamics of Case 1.

### 3.1.2 Case 2: Generation outage of 2.46 GW involving CH and Germany (DE)

To accommodate (achieve) the loss of the target power in this case, generators CH_911689_1, DE_913783_1, and DE_914278_99, were considered to be suddenly tripped, and the system behavior observed in simulation is shown in Fig. 3.3.

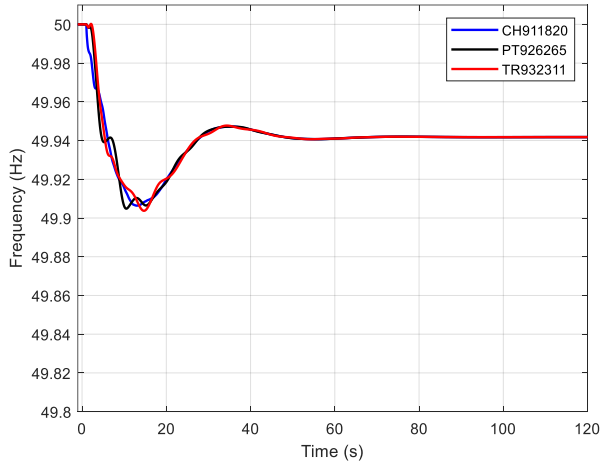


Fig. 3.3 Frequency dynamics of Case 2.

### 3.1.3 Case 3: Generation outage of 4.13 GW involving DE and France (FR)

As for this case, generators referred to as DE_913783_1, DE_914278_99, FR_918204_1, and FR_918203_1 were chosen, and the system response to a sudden disconnection of all of them is given in Fig. 3.4.

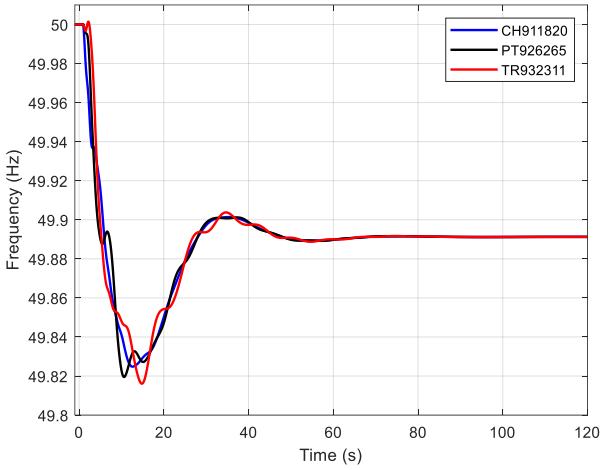


Fig. 3.4 Frequency dynamics of Case 3.

### 3.1.4 Case 4: Load disconnection/reconnection of 3 GW (DE and FR)

First, to achieve the target power here, the loads identified as DE_913058_99, DE_915387_99, FR_918633_99, FR_919778_99, FR_920210_99, FR_918353_99, and FR_918446_99 were selected. Then, the sudden disconnection of these loads was assumed at 1 s of simulation time, and all of them were reconnected simultaneously later at 175 s. The concurrent disconnection/reconnection of these components was adopted as potential situation for the unintentional manipulation of cloud aggregated assets. System performance under these events is shown in Fig. 3.5.

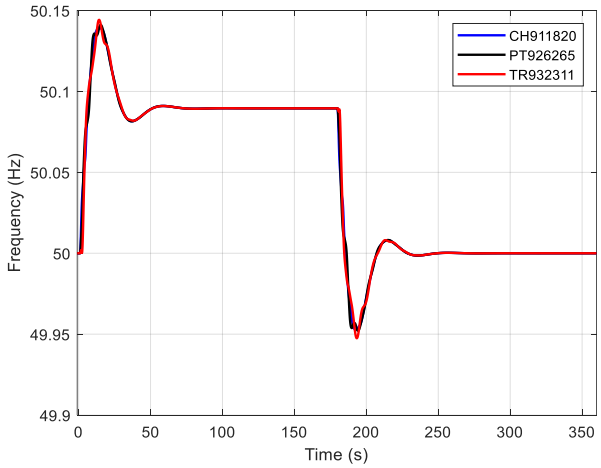


Fig. 3.5 Frequency dynamics of Case 4.

### 3.1.5 Case 5: Load step increase of 3 GW involving loads in Case 4

The same loads in Case 4 are also taken into account here to apply the desired load step increase. Simulation results related to this disturbance are shown in Fig. 3.6.

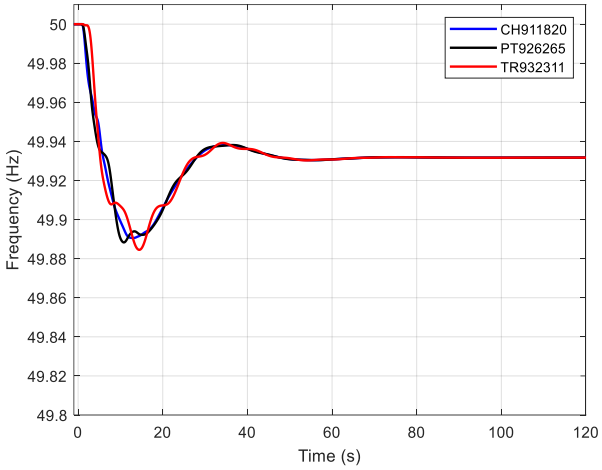


Fig. 3.6 Frequency dynamics of Case 5.

### 3.1.6 Case 6: Load disconnection/reconnection of 3 GW spread over GE, FR, Austria (AT), Netherlands (NL), CH, and Belgium (BE)

In this case, the target power was distributed among six countries (instead of only two as in Case 4) and the loads involved were DE_914296_99, DE_913848_99, FR_919017_99, FR_920198_99, AT_910413_99, NL_925056_99, NL_925175_99, CH_911851_99, BE_910802_99, BE_910820_99, BE_910816_99, and BE_910794_99. By applying the related events at the same time instants as already specified in Case 4, the simulation results in Fig. 3.7 were obtained.

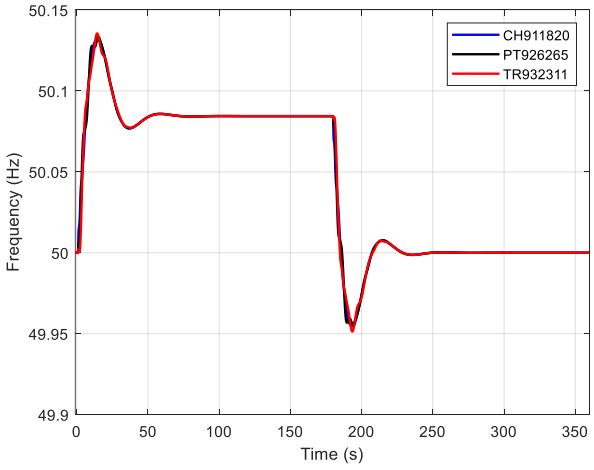


Fig. 3.7 Frequency dynamics of Case 6.

### 3.1.7 Case 7: Load step increase of 3 GW involving loads in Case 6

The same loads defined in Case 6 were used here to apply the indicated load step increase. Simulation results in this regard are shown in Fig. 3.8.

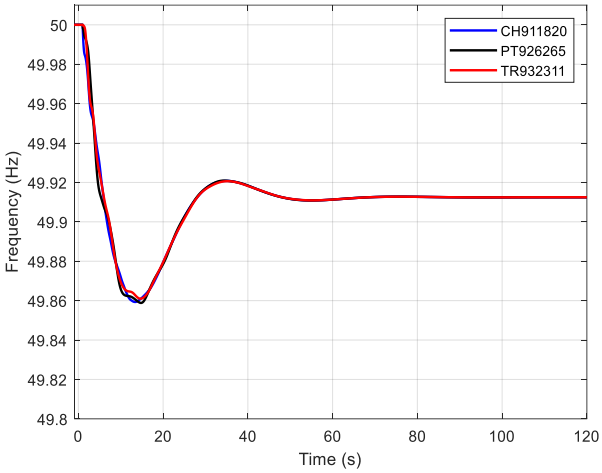


Fig. 3.8 Frequency dynamics of Case 7.

### 3.1.8 Case 8: Load step increments from 3 to 24 GW and distributed across all modelled grids

In order to investigate the effect that the relative load increment size may have on system performance, different load steps from 3 to 24 GW were considered. For this purpose, target load changes were defined, and the desired amounts were then proportionally and randomly accommodated through 27 modelled grids within ±1% of the specified value. Table I shows some examples of how the load was distributed in this way. Resultant frequency dynamics are illustrated in Fig. 3.9.

Table I. Sample distribution of load changes for Case 8.

| **Grid name** | **Target load step increase in MW** | | |
|---|---|---|---|
| | **18,000** | **21,000** | **24,000** |
| Bosn. & Herz. (BA) | 105.25 | 122.25 | 139.32 |
| Serbia (RS) | 277.07 | 320.47 | 368.36 |
| Slovakia (SK) | 177.00 | 218.00 | 243.80 |
| Bulgaria (BG) | 233.94 | 273.63 | 313.90 |
| Austria (AT) | 55.00 | 63.99 | 73.99 |
| Switzerland (CH) | 352.65 | 406.85 | 473.85 |
| Italy (IT) | 1449.91 | 1672.72 | 1927.31 |
| Slovenia (SI) | 87.00 | 103.36 | 116.59 |
| Spain (ES) | 1644.90 | 1905.17 | 2173.52 |
| France (FR) | 3050.10 | 3595.52 | 4115.61 |
| Portugal (PT) | 325.54 | 386.49 | 438.36 |
| Greece (GR) | 354.61 | 420.48 | 479.49 |
| Netherlands (NL) | 710.33 | 832.25 | 940.04 |
| Poland (PL) | 1017.14 | 1186.59 | 1370.02 |
| Germany (DE) | 3496.18 | 4127.71 | 4678.15 |
| Denmark (DK) | 112.34 | 130.24 | 149.38 |
| Belgium (BE) | 568.70 | 639.80 | 708.69 |
| Luxembourg (LU) | 41.65 | 44.54 | 53.40 |
| Czech Republic (CZ) | 405.79 | 468.19 | 541.20 |
| Albania (AL) | 88.89 | 105.79 | 119.79 |
| Croatia (HR) | 152.14 | 177.34 | 203.27 |
| Hungary (HU) | 278.86 | 324.97 | 373.84 |
| Montenegro (ME) | 40.39 | 46.59 | 53.05 |
| Macedonia (MK) | 76.39 | 89.59 | 101.69 |
| Romania (RO) | 349.35 | 408.89 | 463.14 |
| Turkey (TR) | 2244.75 | 2601.69 | 3018.46 |
| European Union Interface (EU) | 300.00 | 350.00 | 357.00 |
| **Total** | **17,995.98** | **21,023.25** | **23,995.34** |

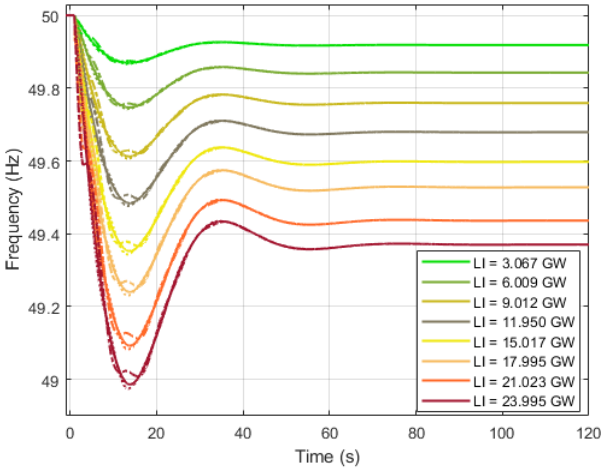


Fig. 3.9 Frequency dynamics of Case 8.

### 3.1.9 Case 9: Load step increments from 3 to 24 GW and distributed only across 14 modelled grids

Similar to Case 8, different system load increments were defined between 3 and 24 GW. However, these changes were proportionally and randomly distributed here only across 14 grids (instead of 27, as in Case 8). The distribution of load in this case is exemplified in Table II. The obtained simulation results are shown in Fig. 3.10.

Table II. Sample distribution of load changes for Case 9.

| **Grid name** | **Target load step increase in MW** | | |
|---|---|---|---|
| | **18,000** | **21,000** | **24,000** |
| Serbia (RS) | 314.01 | 367.37 | 420.94 |
| Slovakia (SK) | 218.00 | 239.80 | 283.00 |
| Austria (AT) | 63.00 | 73.00 | 85.00 |
| Switzerland (CH) | 400.44 | 471.73 | 530.55 |
| Italy (IT) | 1628.02 | 1921.01 | 2185.30 |
| Spain (ES) | 1869.76 | 2194.16 | 2514.23 |
| France (FR) | 3482.86 | 4082.17 | 4692.53 |
| Greece (GR) | 406.88 | 475.21 | 538.00 |
| Netherlands (NL) | 801.21 | 936.55 | 1070.81 |
| Poland (PL) | 1158.04 | 1361.96 | 1549.59 |
| Germany (DE) | 4011.57 | 4623.23 | 5327.60 |
| Belgium (BE) | 555.90 | 724.89 | 834.00 |
| Czech Republic (CZ) | 463.50 | 535.69 | 616.70 |
| Turkey (TR) | 2540.07 | 3002.75 | 3395.43 |
| **Total** | **17,913.26** | **21,009.57** | **24,043.68** |

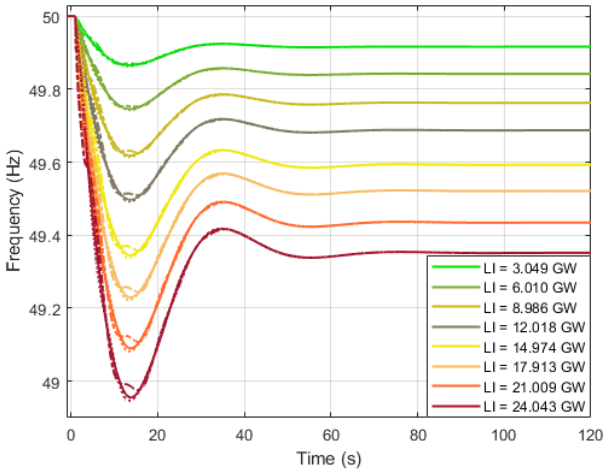


Fig. 3.10 Frequency dynamics of Case 9.

### 3.1.10 Case 10: Load step increase of 3 GW and 6 GW, and reserves limited to 3GW

In practice, the primary reserves for the interconnected operation of the study system are limited to 3 GW, according to the normative contingency in Continental Europe [2]. Since active power reserves for primary frequency control are not limited in the ENTSO-E initial dynamic model, these reserves were limited here to the reference value in order to obtain a more realistic system response under power imbalances caused by load step changes of 3 GW and 6 GW (distributed as in Case 9). Obtained results for these events are respectively illustrated in Fig. 3.11 and Fig. 3.12.

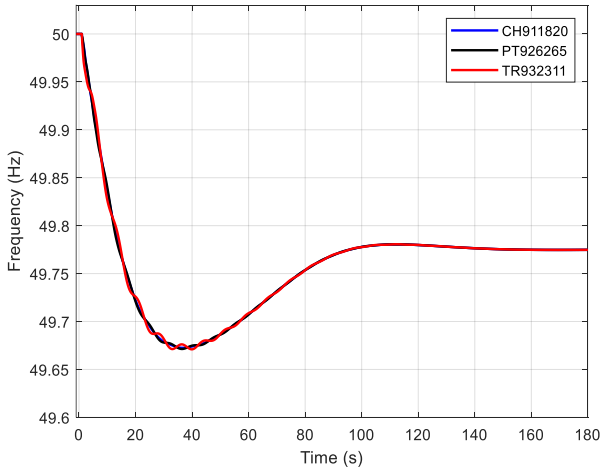


Fig. 3.11 Case 10: 3 GW load step increment.

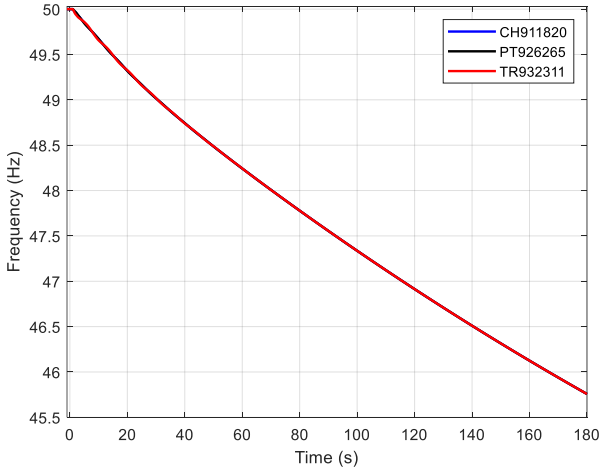


Fig. 3.12 Case 10: 6 GW load step increment.

### 3.1.11 Case 11: Load disconnection/reconnection of 3 GW and 6 GW, and reserves limited to 3GW

With primary reserves limited to 3 GW, the system response to the disconnection of 3 GW of load at 1 s, and its reconnection at 175 s is provided in Fig. 3.13. On the other side, Fig. 3.14 shows corresponding results for a load disconnection event of 6 MW. Selected loads to achieve target power were taken from related incidents in Case 9.

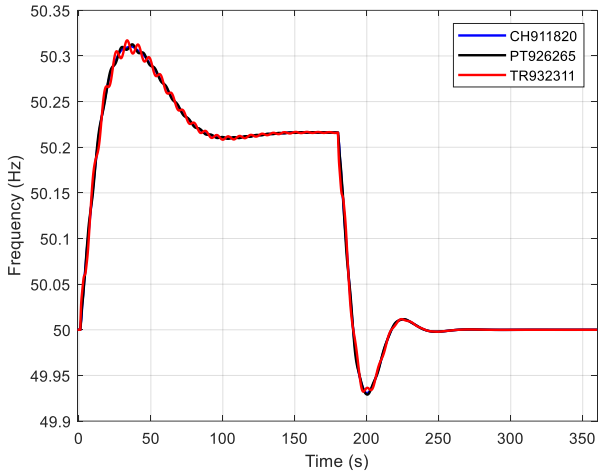


Fig. 3.13 Case 11: ±3 GW step change.

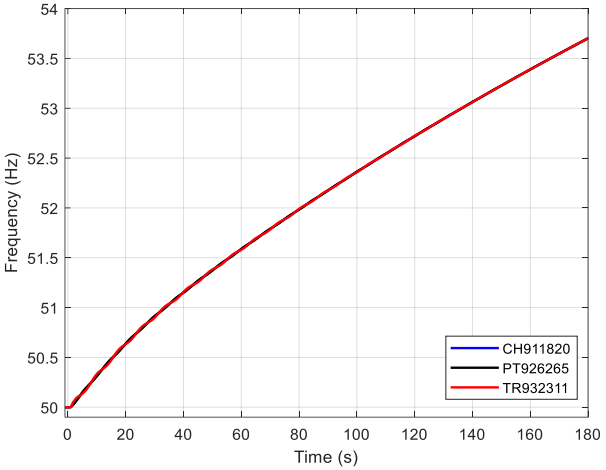


Fig. 3.14 Case 11: 6 GW load disconnection.

### 3.1.12 Case 12. Generation loss of 2.6 GW and 4.1 GW, and reserves limited to 3GW

With the disconnection of the generators considered in Case 1, and limiting the primary reserves to 3 GW, the frequency dynamics of the study system are illustrated in Fig. 3.15. On the other hand, Fig. 3.16 provides corresponding results for a generation loss event of 4.1 GW with a selected set of generators as in Case 3.

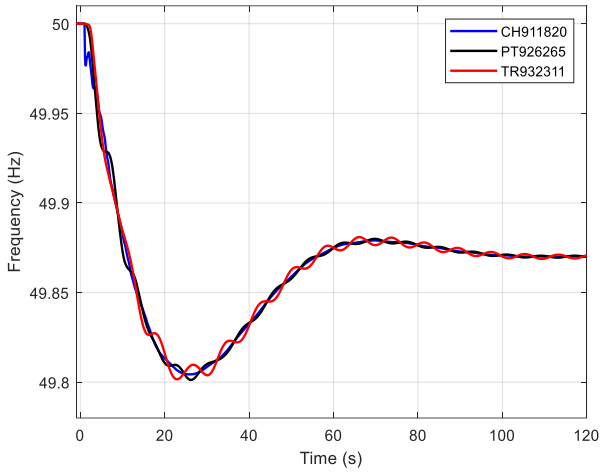


Fig. 3.15 Case 12: 2.6 GW generation loss.

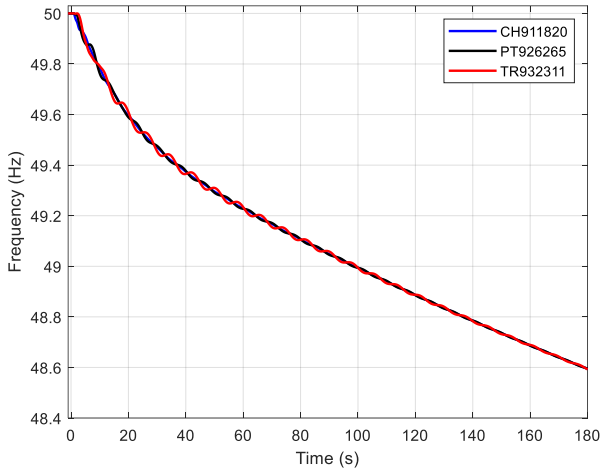


Fig. 3.16 Case 12: 4.1 GW generation loss.

### 3.1.13 Case 13: Load step increase of 24 and 100 GW without/with reserve limits

The case where a sudden load increment of 24 GW is applied at 1s with no limitation in active power reserves (NRL) and with these ones limited to 3 GW is considered here. With the respective load distribution as indicated in Table II of Case 9, obtained simulation results of this event are provided in Fig. 3.17 through the frequency dynamics of a representative bus in Switzerland. In addition, a load step increment of 100 GW under the same conditions was also applied, and the resultant system response is illustrated in Fig. 3.18. The load distribution of this change was also carried out in a proportional and random way across the countries included in Table II.

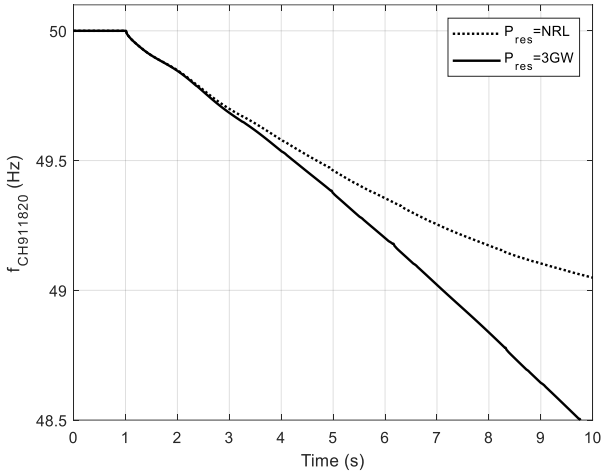


Fig. 3.17 Case 13: Load step increase of 24 GW.

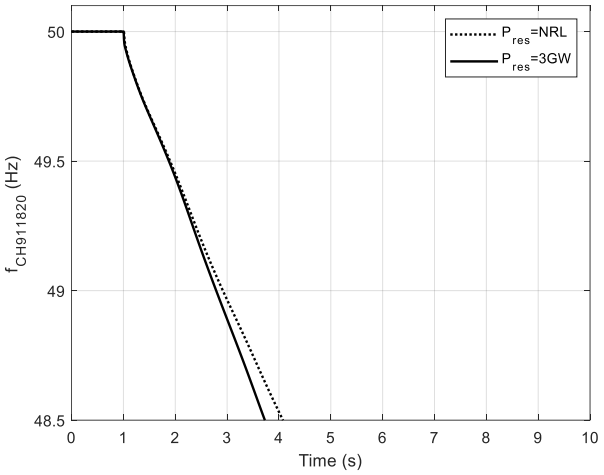


Fig. 3.18 Case 13: Load step increase of 100.

### 3.1.14 Case 14: Disconnection of IT and CH from the rest of the system

System splits may result in very critical events in terms of power imbalance [9]-[12], depending on the loading and generation conditions of the network. Since several incidents related to grid splits have already occurred in Continental Europe, an event consisting in the separation of Italy and Switzerland from the rest of the system is considered here for further analysis, as represented in Fig. 3.19. This study case was pointed out as of great interest by Swissgrid partner due to the significant amount of power imported by Italy through Switzerland and the potential implications during a system split. For this case, the initial operating point of the study system was modified to obtain the generation and load conditions in Table III regarding the grids of Switzerland, Italy, and Germany.

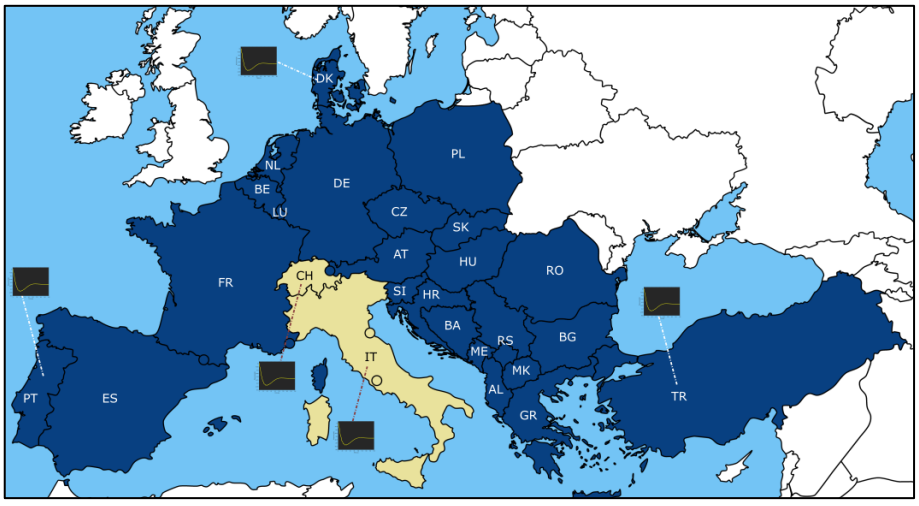


Fig. 3.19 Representative region to be islanded (in beige color).

Table III. Generation and load conditions for CH, IT, and DE before the event.

| Grid name | GW | | |
|---|---|---|---|
| | Generation | Load | Import |
| Switzerland (CH) | 6.84 | 8.96 | 2.23 |
| Italy (IT) | 27.03 | 36.68 | 9.94 |
| Germany (DE) | 98.53 | 89.34 | -7.87 |

To achieve new steady state operating conditions and attain a constant electrical frequency from the beginning of the simulation, the initial operating point of governor models in selected generators of the German grid was correspondingly adjusted to match the power flows resultant from the conditions in Table III. Then, the response of the test system under the considered event is shown in Fig. 3.20.

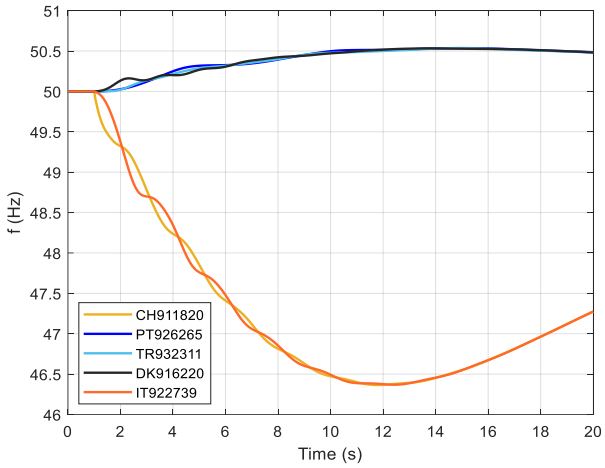


Fig. 3.20 Case 14: separation of IT and CH grids.

### 3.1.15 Case 15: Disconnection of FR, ES, and PT from the rest of the system

The split of the system into two parts is also considered here but, in this case, France, Spain, and Portugal are assumed to be separated together, as illustrated in Fig. 3.21 (as recommended by Swissgrid partner). The original operating point of the study system was also changed in such a way that generation and load conditions for the grids of France, Spain, Portugal, and Germany were adjusted to the values given in Table IV (after load flow computations).

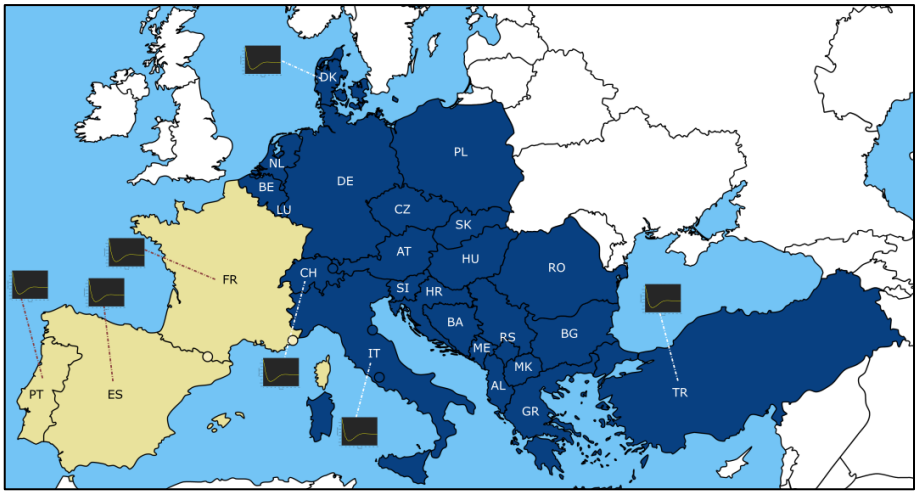


Fig. 3.21 Representative region to be islanded (in beige color).

Table IV. Generation and load conditions for PT, ES, FR, and DE before the event.

| Grid name | GW | | |
|---|---|---|---|
| | Generation | Load | Import |
| Portugal (PT) | 8.29 | 8.35 | 0.22 |
| Spain (ES) | 38.43 | 41.77 | 3.93 |
| France (FR) | 75.31 | 78.14 | 5.03 |
| Germany (DE) | 108.72 | 89.34 | -17.26 |

To achieve new initial steady state operating conditions, the initial output of the governor models associated with a set of generators of the German grid was also modified. In addition, the reactive power of several loads in France was also altered to avoid a significant increment of corresponding bus voltages after system split. The obtained system frequency response for the considered event is illustrated in Fig. 3.22.

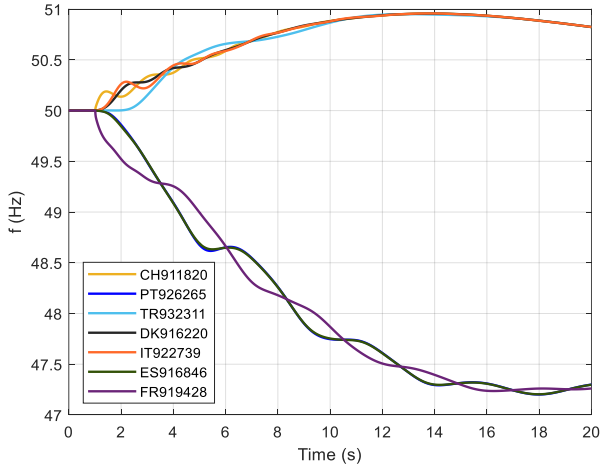


Fig. 3.22 Frequency dynamics under disconnection of FR, ES, and PT.

## 3.2 Scenarios for future conditions of the system

In order to be able to investigate the system frequency behavior for possible future scenarios, different variations in terms of reduction of overall system inertia were implemented in the study system. Such variations were considered for the representation of the future development of the grid regarding potential penetrations levels of renewable energy resources interfaced through power electronics converters. For illustrative purposes, different percentages of overall inertia reduction such as 30%, 50% and 70% were assumed for analysis. In this way, the system response associated for example with the load step increases of 24 GW and 100 GW without/with reserve limits (Case 13) is shown in Fig. 3.23 and Fig. 3.24, respectively. Now, since system splits may give place to very critical power imbalances due to high power transfers on inter-tie transmission lines and available inertia, the grid separation events described in Cases 14 and 15 of Section 3.1 were also selected here for further analysis. As for this, related simulation results of the islanded systems during the first instants of the incident and under aforementioned overall inertia reductions are provided in Fig. 3.25 and Fig. 3.26.

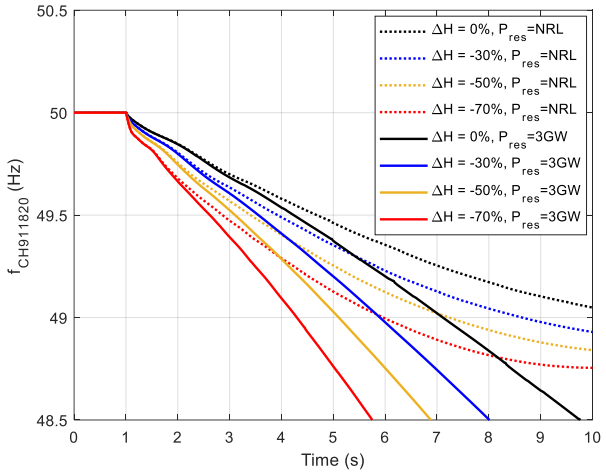


Fig. 3.23 $\Delta P_{load}$=24GW without/with reserve limits.

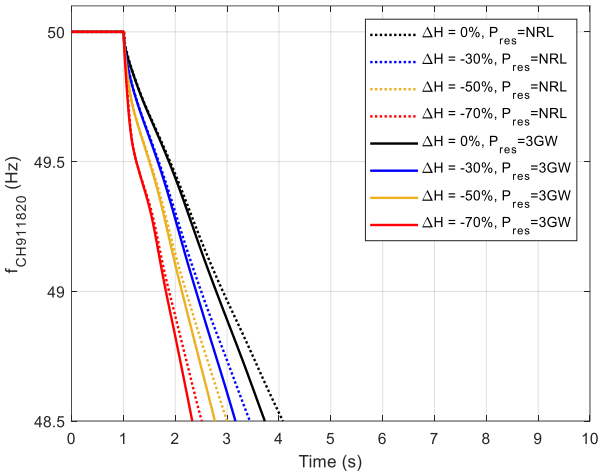


Fig. 3.24 $\Delta P_{load}$=100 GW without/with reserve limits.

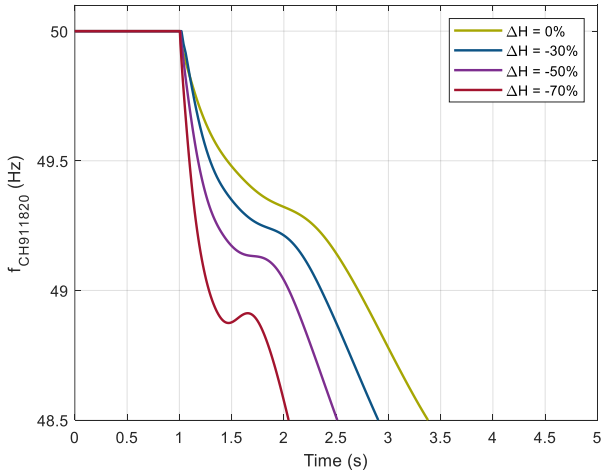


Fig. 3.25 Disconnection of CH and IT.

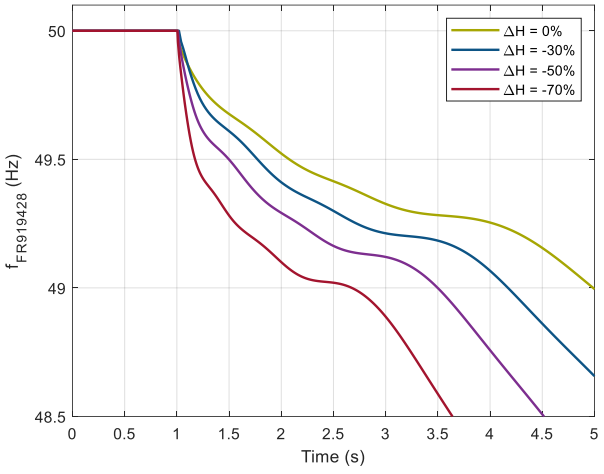


Fig. 3.26 Disconnection of FR, ES, and PT.

## 3.3 Quantification of malfunctions caused by aggregated electrical assets

In order to quantify the impact of related power imbalances on the frequency stability of the study system, a summary of the results from the extensive number of simulations performed is presented here. With the active power reserves as originally included in the model, Fig. 3.27 and Fig. 3.28 respectively provide the computed RoCoF at 500 ms (as commonly considered [13]) and the nadir of frequency for different load step increments and system inertia variations. From Fig. 3.27, it can be observed that the RoCoF remains below 0.4 Hz/s for the several inertia reductions and load changes considered. Now, concerning the frequency deviations represented in Fig. 3.28, the 24 GW load increment example indicates that all involved inertia variations for this case will bring about the intervention of load shedding since $\Delta f > 1$ Hz (frequency nadirs below 49 Hz). By including the limitation of reserves to 3 GW, the RoCoF is correspondingly affected as graphically revealed in Fig. 3.29. For comparative purposes, the RoCoF values with and without the limitation of active power reserves to 3 GW are provided in Table V. Since corresponding results are very comparable (with only small differences), it can be concluded from the computations that the RoCoF at 500 ms is practically the same in both illustrated cases.

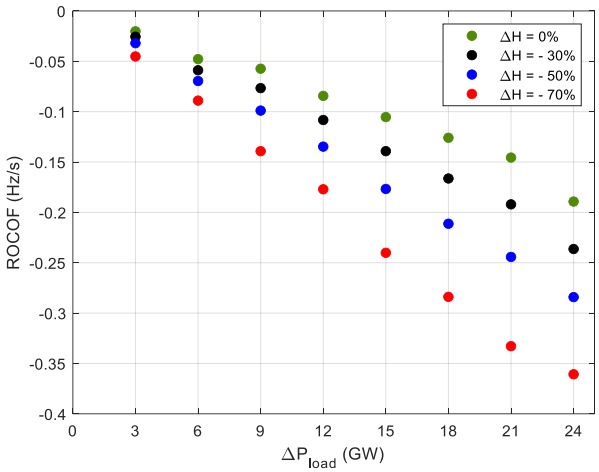


Fig. 3.27 RoCoF with active power reserves as originally included.

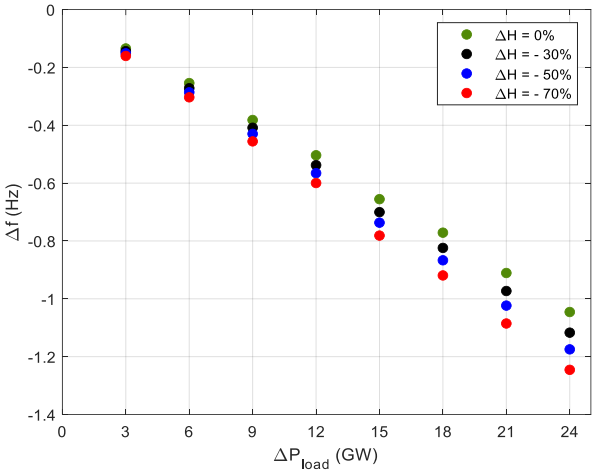


Fig. 3.28 Δf at nadir with active power reserves as originally included

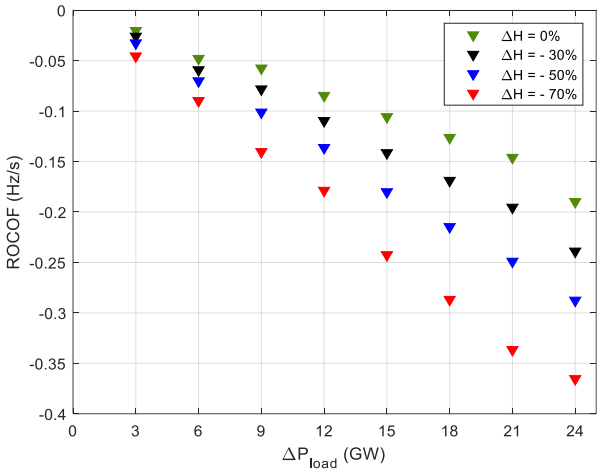


Fig. 3.29 RoCoF with active power reserves limited to 3GW.

Table V. Comparison of RoCoF values.

| $\Delta P_{load}$ (MW) | Limited reserves | RoCoF (Hz/s) at 500 ms | | | |
|---|---|---|---|---|---|
| | | ΔH=0% | ΔH=-30% | ΔH=-50% | ΔH=-70% |
| 3 | No | 0.020 | 0.025 | 0.032 | 0.045 |
| | Yes | 0.020 | 0.025 | 0.032 | 0.045 |
| 6 | No | 0.047 | 0.058 | 0.069 | 0.089 |
| | Yes | 0.047 | 0.059 | 0.070 | 0.089 |
| 9 | No | 0.057 | 0.076 | 0.098 | 0.139 |
| | Yes | 0.057 | 0.078 | 0.101 | 0.140 |
| 12 | No | 0.084 | 0.108 | 0.134 | 0.177 |
| | Yes | 0.084 | 0.109 | 0.136 | 0.178 |
| 15 | No | 0.105 | 0.139 | 0.176 | 0.240 |
| | Yes | 0.105 | 0.141 | 0.180 | 0.242 |
| 18 | No | 0.125 | 0.166 | 0.211 | 0.283 |
| | Yes | 0.126 | 0.168 | 0.214 | 0.286 |
| 21 | No | 0.145 | 0.192 | 0.244 | 0.332 |
| | Yes | 0.146 | 0.195 | 0.249 | 0.336 |
| 24 | No | 0.189 | 0.236 | 0.284 | 0.360 |
| | Yes | 0.189 | 0.238 | 0.287 | 0.365 |

Regarding the simulated grid split scenarios, Table VI and Table VII provide the computed numerical values of the RoCoF for the variations in system inertia. According to the obtained results, RoCoF values greater than 1 Hz/s are observed for all the considered inertia reductions in the particular case of the islanded grid consisting of Switzerland and Italy.

Table VI. RoCoF in the islanded system consisting of Switzerland and Italy.

| RoCoF at 500 ms (Hz/s) | | | |
|---|---|---|---|
| ΔH=0% | ΔH=-30% | ΔH=-50% | ΔH=-70% |
| -1.042 | -1.301 | -1.656 | -2.246 |

Table VII. RoCoF in the islanded system consisting of France, Spain and Portugal.

| RoCoF at 500 ms (Hz/s) | | | |
|---|---|---|---|
| ΔH=0% | ΔH=-30% | ΔH=-50% | ΔH=-70% |
| -0.6472 | -0.7806 | -1.0018 | -1.4368 |

According to the dynamic response of the study system, during interconnected operation and without limiting the reserves, the application of several load step increments shows that imbalances around 24 GW may lead to frequency nadirs under 49 Hz, which in turn would cause the activation of load shedding schemes. In addition, since a comparable frequency response was obtained either by distributing the collective load changes across the twenty-seven modelled grids or only across fourteen of them, the last approach was used for the sake of reducing the computational effort in the preparation and simulation of further related scenarios.

Now, the simulations studies with the primary frequency control reserves limited to 3 GW provide a more realistic system response. In this case, after and imbalance event of 3 GW for example, the system remains stable but the transient and steady state frequency deviations become larger as compared to the performance with no reserve limitation (NRL). Furthermore, a load step increment of 6 GW will endanger the frequency stability of the grid with only 3 GW of available reserves, as derived from the simulation results. It is important to clarify here that since underfrequency load shedding functions are not modelled in the IDMCE, frequency deviations that grow indefinitely are obtained after the aforementioned disturbance.

In general, from the simulation results with the reserves conditioned to 3 GW, it can be inferred that any sudden network imbalance that exceeds the reference amount will lead to growing frequency deviations

and consequently to the system collapse if no appropriate countermeasures are taken. On the other hand, regarding RoCoF values computed at 500 ms after increasing load step changes, it can be deduced that they are relatively small during interconnected operation, as compared to the critical value of 1 Hz/s specified in [13]. Based on extensive time domain simulation analysis with current system inertia, it can be said that as long as the system is interconnected the referred frequency gradients can remain within admissible values even for a significant imbalance between generation and load such as 100 GW. However, for some scenarios involving system separation, the RoCoF may reach or even exceed the critical value, as revealed by the study case related to the disconnection of Switzerland and Italy from the rest of the system.

Further investigation of system frequency performance under potential low inertia scenarios showed that RoCoF values for a load step change of 24 GW for example are well below the reference limit. Besides, among the three considered reduction cases of system inertia (30%, 50% and 70%), only the 70% reduction case in the 100 GW load increase incident seems to cause a frequency gradient slightly greater than 1 Hz/s. On the other hand, regarding the grid split scenario involving the islanding of Switzerland and Italy under potential future conditions, the results indicate that the base case, as well as the overall system inertia reductions from that, will lead to RoCoFs at 500 ms greater than 1 Hz/s, according to the measured frequency. In fact, a value of more than 2 Hz/s was identified for the 70% reduction example. As for the study case where France, Spain, and Portugal are separated from the system, it was observed that particular inertia reductions of approximately 50% and greater ones will give place to frequency gradients of more than 1 Hz/s there.

# 4 Experimental frequency dynamic support under system splits

In general, system splits may expose parts of the grid to severe operating conditions that lead to uncontrolled cascading outages and the supply interruption of a significant amount of load. Particularly, in islands with insufficient generation reserve, the frequency may start to decline quickly and reach some levels that cause the trip of generating units, aggravating the situation even more. Then, automatic islanding detection becomes imperative to try to appropriately deal with the resultant isolated subsystems so that resynchronization of them and restoration of the whole system can be accomplished as fast as possible.

Moreover, due to the foreseen impacts of system splits on the resilience of the Continental Europe Synchronous Area under low inertia scenarios, ENTSO-E announced “Project Inertia-Phase II” in the year 2023 [14], which aims to improve current methodologies to assess split cases (based on long-term future conditions) and propose concrete measures to address related frequency stability challenges. As part of this initiative, and with the intention to limit the likelihood and consequences of system splits, a first report has already been released [14] with a series of identified measures to enhance system resilience. Within this context, the requirement of additional support functions to limit the nadir/zenith of frequency (LFSM-UC/LFSM-O) by new grid users is categorized as an effective and practical measure to be considered. Specifically, through the LFSM-O function, inverter coupled generators can quickly reduce their injected active power when the frequency overpasses a given threshold above the nominal value. On the other hand, with the LFSM-UC capability, inverter coupled loads can rapidly decrease current power consumption under a given drop frequency.

Given the importance of limiting the potential effects of system splits, a set of activities were included in the IMPALA project with the main goal of demonstrating, evaluating, and testing in the lab, a concept to

determine grid separation based on frequency deviations measured from tiko boxes, which detect such condition and act against the spreading of consequences. Therefore, a lab-scale cyber-physical testbed, based on Hardware-in-the-Loop (HIL) techniques and industrial devices provided by tiko, was proposed, built up, and used for the aforementioned purposes.

## 4.1 Lab-scale setup development

After a common understanding with the industrial partner in terms of main goal, expected setup, and test system model, the lab-scale testbed illustrated in Fig. 4.1 was developed, which consist of multiple equipment available in the Renewable Electrical Energy Laboratory (REE-lab) [15]. As indicated in this figure, a dynamic simulation model of the well-known Kundur power system was considered [16], which comprises two grid areas interconnected by a set of transmission lines. Two generating units, rated at 900 MVA and 20 kV, are included in each area. System generators and loads are set up in such a way that a power of 400 MW is flowing from area 1 to area 2 in the base case scenario. Parameters of the multi-machine system model, including generators, AVRs, transmission lines, loads, and reactive compensation devices, were taken from [16]. The real-time environment of the setup is represented here by main components such as the OPAL-RT's real-time time simulator (where the test system model is run), two 16-channel digital-to-analog converter modules, and the Regatron power amplifier. Moreover, sets of devices consisting of tiko's M-Box, D-Box, and K-Box, were facilitated by the industrial partner to be configured and included in the physical testbed. Each M-Box refers to the controller under test and provides the communication gateway to tiko's private cloud system. The D-Box is basically an energy meter and switch to control decentralized devices. An M-Box is required to connect D-Boxes to the back-end cloud. The K-Box is also a metering and control device that contains a rely for on/off switching. The K-Box is linked to the cloud through the gateway (M-Box). The available devices were arranged as indicated to carry out different tests related to the detection of grid separation based on decentralized frequency deviations.

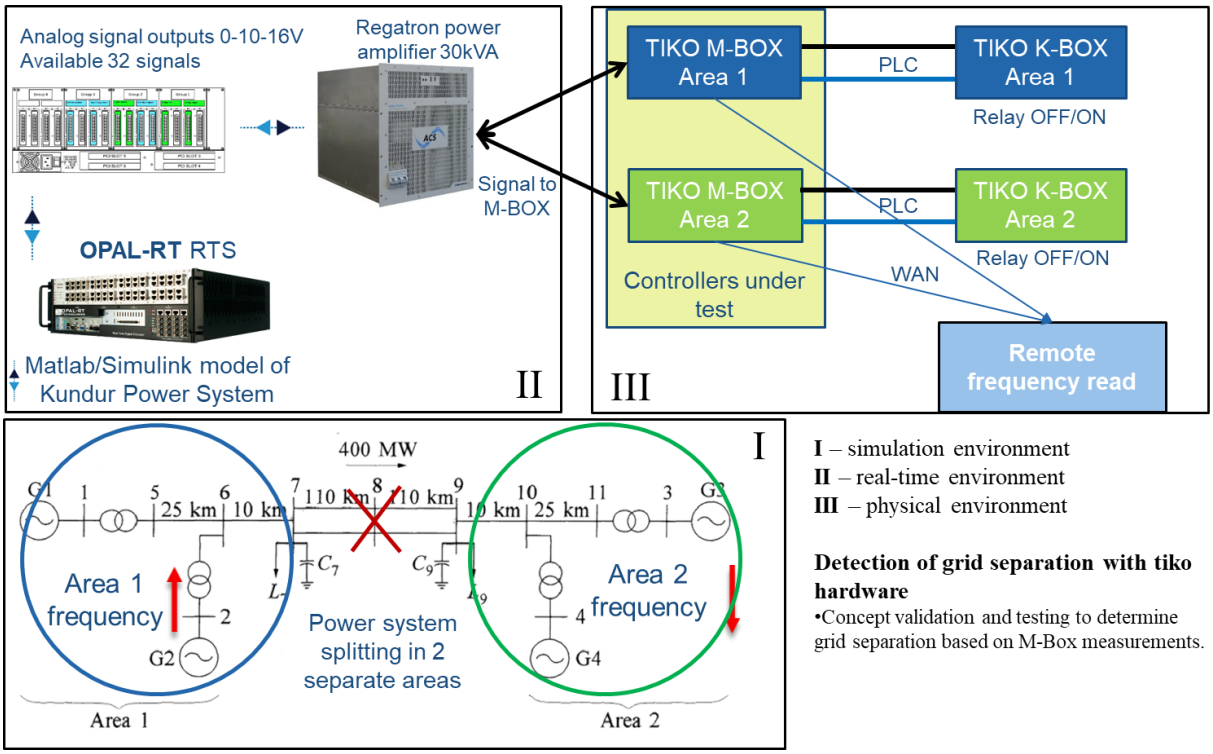


Fig. 4.1 ZHAW REE-Lab IMPALA project testbed.

Details of the test power system model and its implementation in Matlab/Simulink environment for real-time simulation are shown in Fig. 4.2, and the response of the grid during a system split is exemplified in Fig. 4.3.

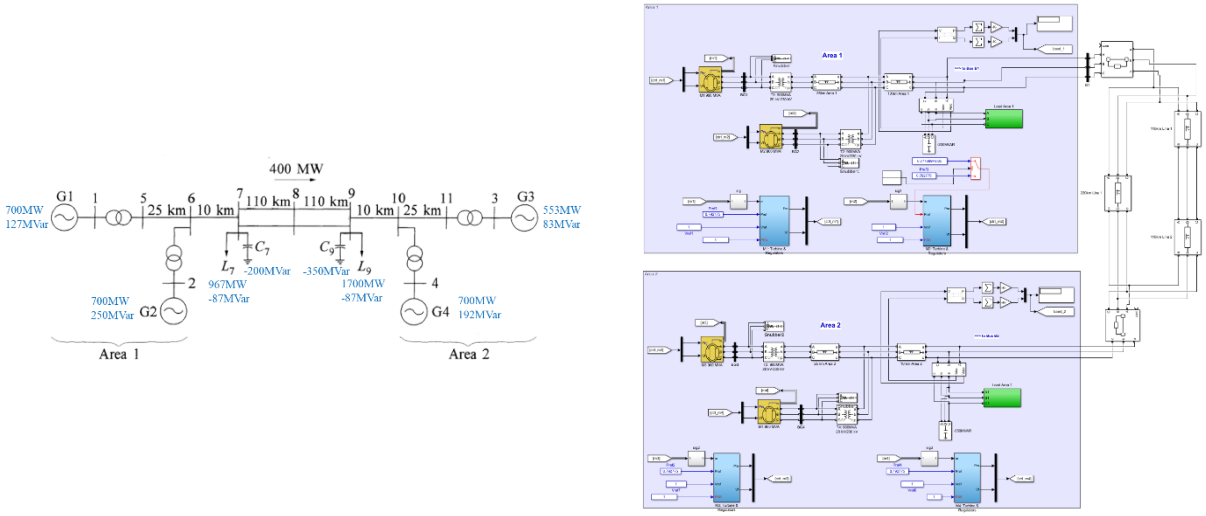


Fig. 4.2 Kundur dynamic model and its representation in Matlab/Simulink simulation environment.

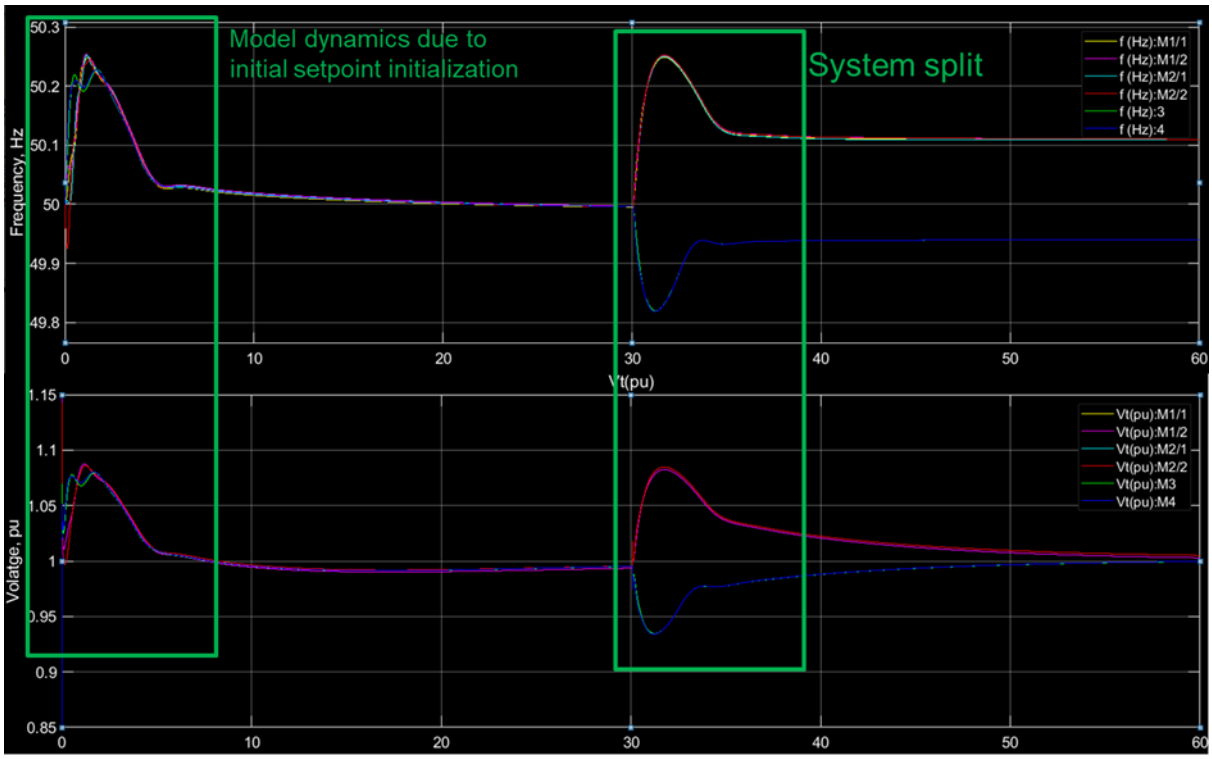


Fig. 4.3 Kundur system frequency/voltage behaviour during system split.

Physical connexion of the M/D/K-Boxes, as accomplished for the lab setup, is illustrated in Fig. 4.4. All three boxes are connected separately to each phase and allow to potentially investigate three asynchronous areas.

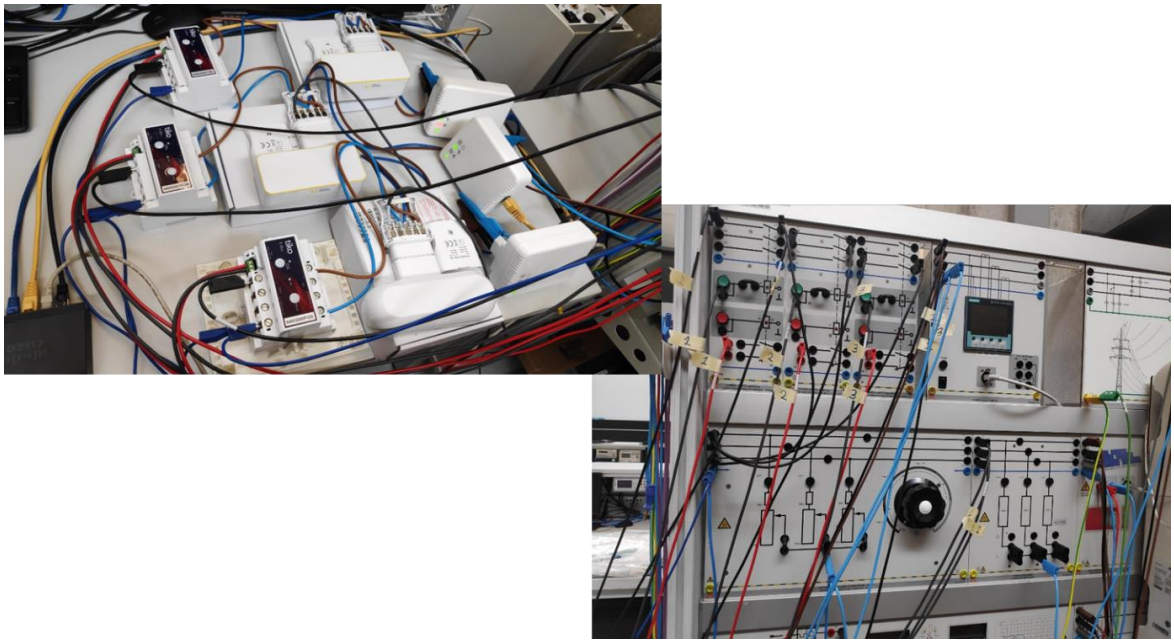

Fig. 4.4 M/D/K-Boxes setup in ZHAW REE-Lab and connection to each phase separately (A/B/C).

The successful pairing of all boxes with tiko cloud is shown in Fig. 4.5. They can be monitored and controlled remotely as shown in Fig. 4.6.


Fig. 4.5 Pairing of tiko boxes with the cloud.

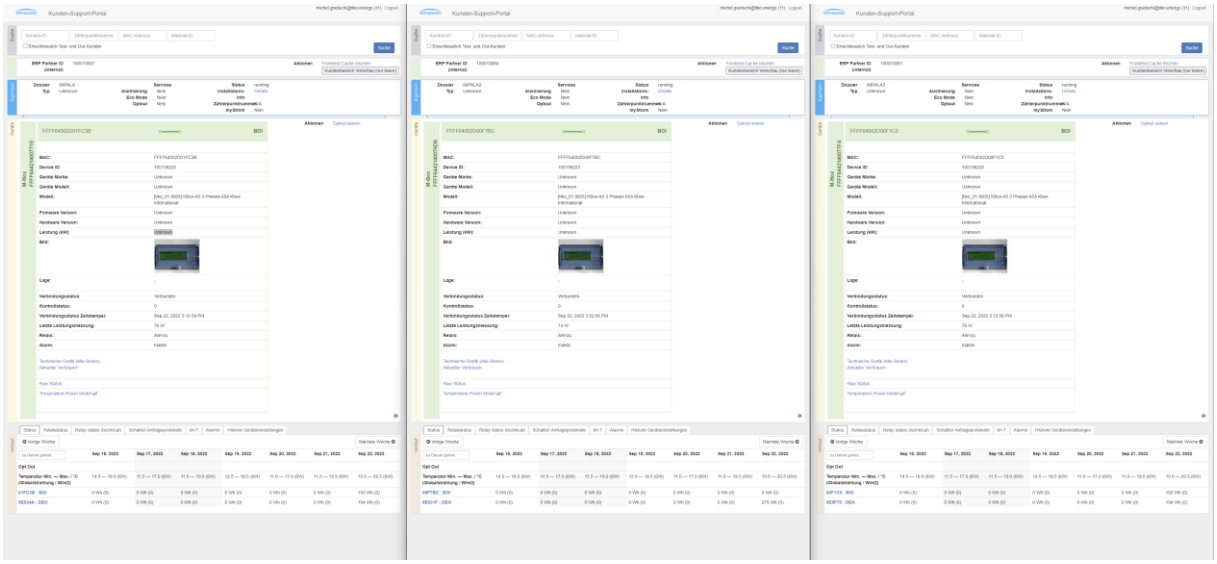

Fig. 4.6 tiko cloud platform and devices under investigation.

## 4.2 Evaluation and testing of devices

After successful deployment of the lab setup, the tests described in the following were performed.

### 4.2.1 Open-loop test (without back loop)

This test was carried out to synchronise recordings of frequencies from the simulation environment and from the field. For this purpose, a system split case with resynchronisation of the isolated subsystems was implemented, and the resultant dynamic response according to frequency measurements from M-boxes is shown in Fig. 4.7. Furthermore, comparison of the system response as seen from tiko boxes and directly from the simulation environment is given in Fig. 4.8 where some differences can be clearly observed.

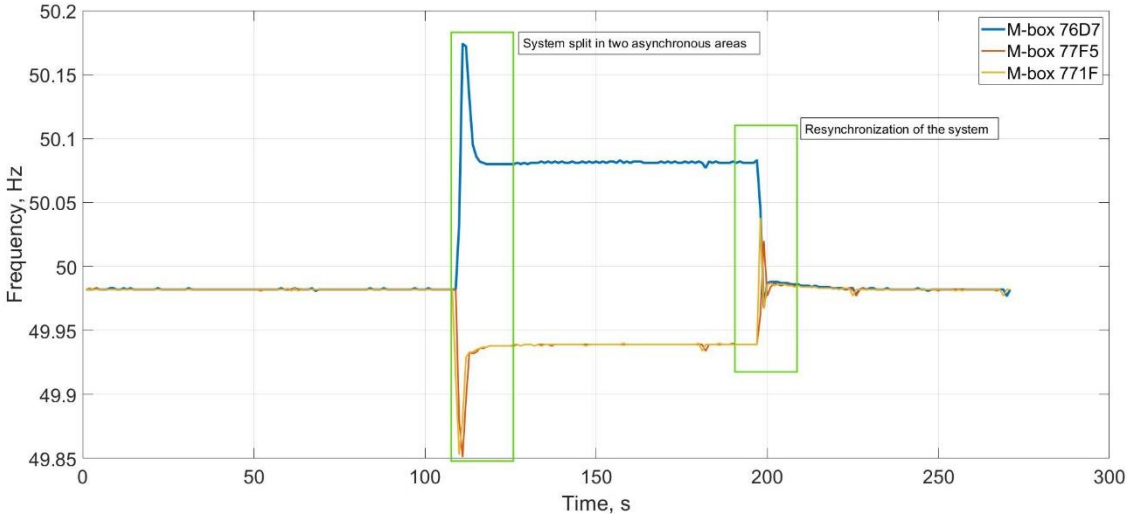


Fig. 4.7 Measurements from tiko M-boxes during open-loop test.

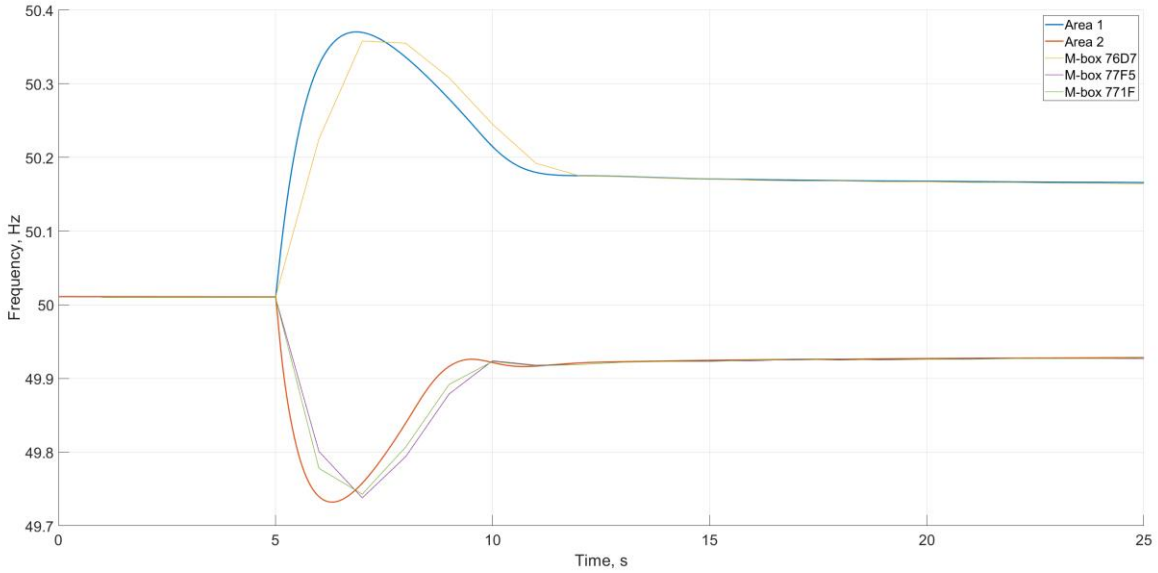


Fig. 4.8 Measurements from tiko M-boxes and simulation environment during open-loop test.

As seen in Fig. 4.8, although the dynamics are comparable in terms of frequency nadir/zenith and final steady-state values after the considered system split, the transient response given by the tiko boxes shows a time shifted behaviour, which has to do with the internal algorithm of the M-Box for frequency estimation and corresponds to approximately 300–400 ms. Based on the obtained results, it was determined that the frequency measured in the M-Box can be accessed internally with a special firmware version, but this is not activated in the hardware that was used in REE-lab. Besides, with the three sets of tiko boxes installed in ZHAW-REE lab, it was not possible to see any reaction with the present implementation of tiko´s algorithm regarding the associated loads.

### 4.2.1 Open loop tests with tiko's decentralized frequency method

In this case, the decentralized frequency approach used in tiko's pool, and illustrated in Fig. 4.9, was implement in Simulink environment.

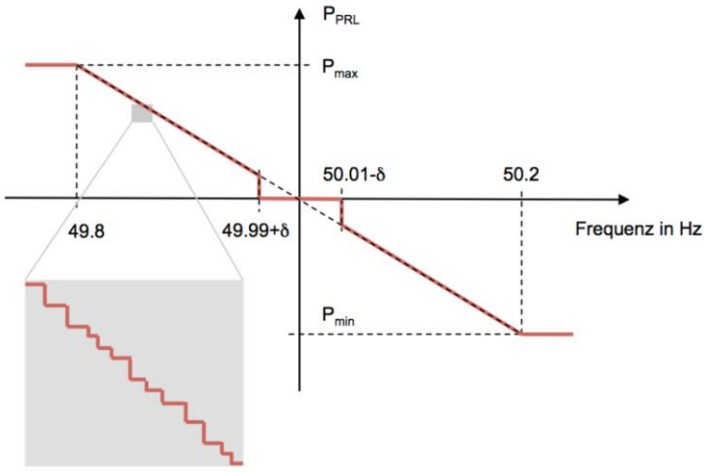


Fig. 4.9 tiko pool decentralized frequency method (figure provided by tiko).

The following aspects can be highlighted as related to the approach in the previous figure:

- A local, decentralized operation mode can be provided, where each installation reacts individually based on the local frequency measurement only.

- In the decentralized operation mode, each installation will be activated or deactivated at maximum power when certain frequency thresholds are reached. No reaction is required within a predefined frequency dead band. Outside 50 Hz +/- 200 mHz, the maximum power of the pool is activated or deactivated and is in compliance with LFSM-U/O.
- In order to guarantee constant power and energy in the pool, the individual trigger frequencies have to change on a regular basis. Each installation updates its trigger frequencies automatically every minute based on a predefined scheme.

Therefore, the Kundur dynamic model was extended with the aforementioned decentralized frequency control method to operate on 218 MW of load, which represents approximately 8% out of a total system load of 2660 MW. The amount of controlled load was distributed into the two areas of the test system, with 36% in Area 1 and 64% in Area 2. In order to observe the impact of system inertia constant (H) variations under scenarios of the given controlled and no controlled load, five study cases were defined for a system split during a power exchange of 330 MW between the two areas. The obtained response for the considered cases is illustrated in Fig. 4.10 (Area 1) and Fig. 4.11 (Area 2).

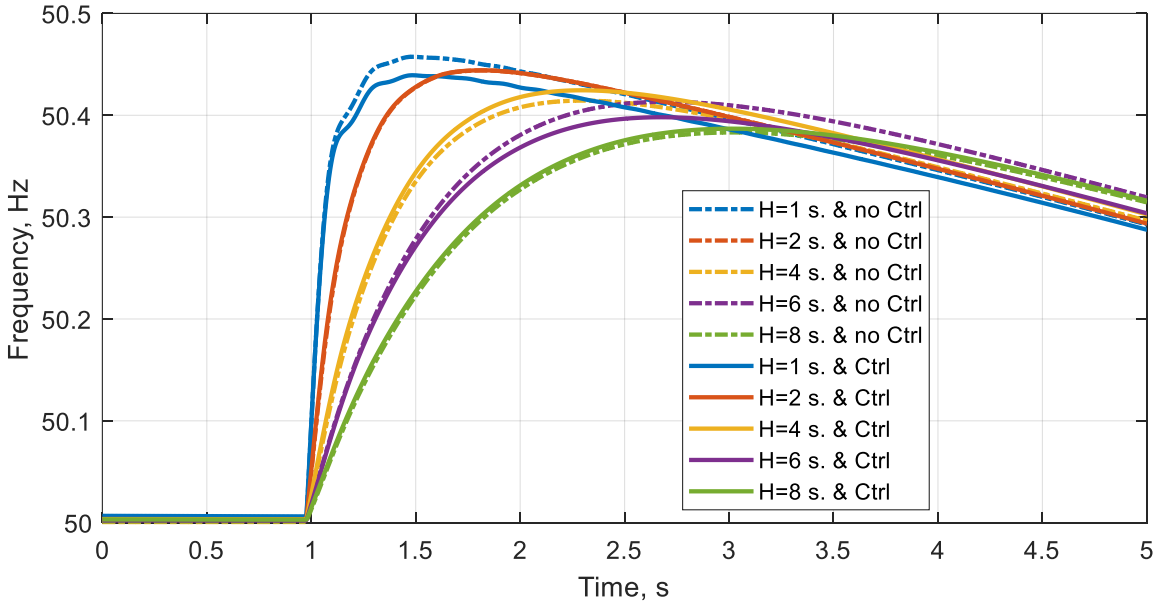


Fig. 4.10 Area 1, frequency dynamics for different inertia cases.

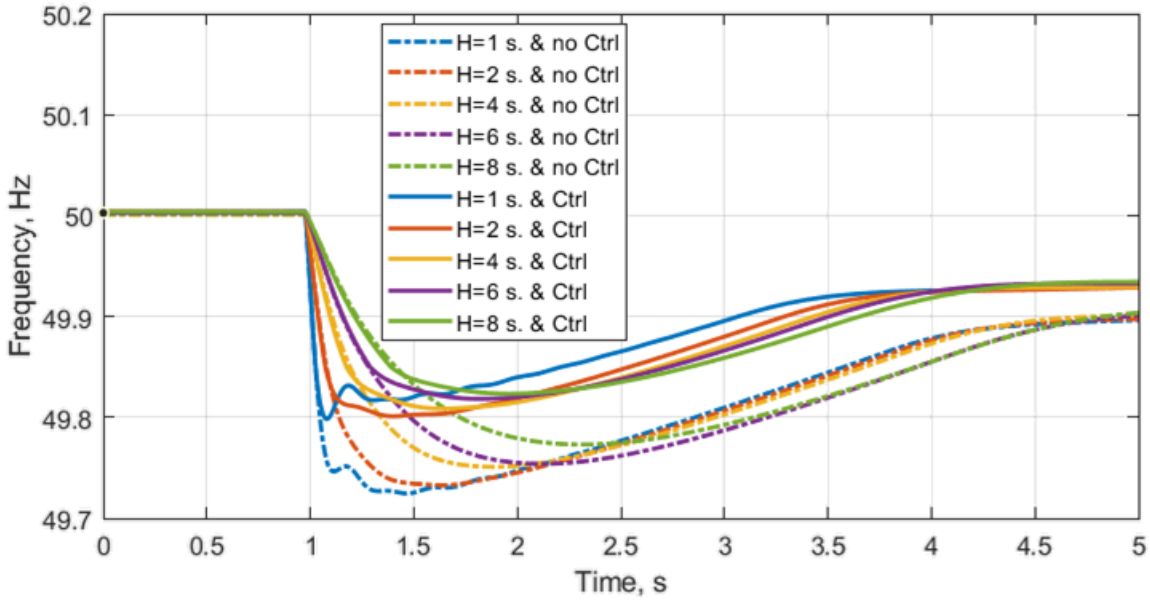


Fig. 4.11 Area 2, frequency dynamics for different inertia cases.

The results of the two previous figures can be summarised as in Table VIII, where improvements in the frequency nadir for the case of load under control can be particularly observed. In any case, it is clear that the ROCOF increases as the equivalent inertia of the system is reduced. In general, the results demonstrate a concept to determine grid separation based on frequency deviations measured from the tiko boxes, which detect a possible problem in the grid and act against its spreading.

Table VIII. Comparison of RoCoF (Hz/s) and Min/Max frequency (Hz) values.

| H, (s) | Area | Without Control | | | | With Control | | | | |
|---|---|---|---|---|---|---|---|---|---|---|
| | | RoCoF at 200 ms | RoCoF at 500 ms | RoCoF at 1000 ms | Min/Max, Hz | RoCoF at 200 ms | RoCoF at 500 ms | RoCoF at 1000 ms | Min/Max, Hz | Δ Min/Max, mHz |
| 8 | Area 1 | 0.44 | 0.43 | 0.32 | 50.38 | 0.44 | 0.44 | 0.32 | 50.39 | 10.00 |
| | Area 2 | 0.51 | 0.33 | 0.22 | 49.77 | 0.38 | 0.33 | 0.18 | 49.82 | -50.00 |
| 6 | Area 1 | 0.73 | 0.53 | 0.37 | 50.41 | 0.69 | 0.53 | 0.36 | 50.40 | -10.00 |
| | Area 2 | 0.63 | 0.41 | 0.25 | 49.76 | 0.62 | 0.36 | 0.18 | 49.82 | -60.00 |
| 4 | Area 1 | 0.85 | 0.65 | 0.41 | 50.41 | 0.87 | 0.66 | 0.41 | 50.43 | 20.00 |
| | Area 2 | 0.78 | 0.45 | 0.25 | 49.75 | 0.72 | 0.39 | 0.18 | 49.81 | -60.00 |
| 2 | Area 1 | 1.68 | 0.85 | 0.44 | 50.44 | 1.48 | 0.84 | 0.44 | 50.45 | 10.00 |
| | Area 2 | 1.11 | 0.54 | 0.26 | 49.73 | 0.92 | 0.40 | 0.18 | 49.80 | -70.00 |
| 1 | Area 1 | 1.87 | 0.92 | 0.43 | 50.47 | 1.89 | 0.86 | 0.42 | 50.46 | -10.00 |
| | Area 2 | 1.20 | 0.56 | 0.25 | 49.72 | 0.91 | 0.38 | 0.16 | 49.84 | -120.00 |

Further tests were carried out under controlled load cases and system inertia constant values variations in order to examine the system response when the load reaction time is varied (time necessary to estimate frequency via tiko M-Boxes, send signals to D/K-Boxes, and operate the load). For study purposes, a delay of 500 ms between frequency measurement and load activation was considered. Obtained system dynamics corresponding to Area 1 and Area 2 are respectively presented in Fig. 4.12 and Fig. 4.13.

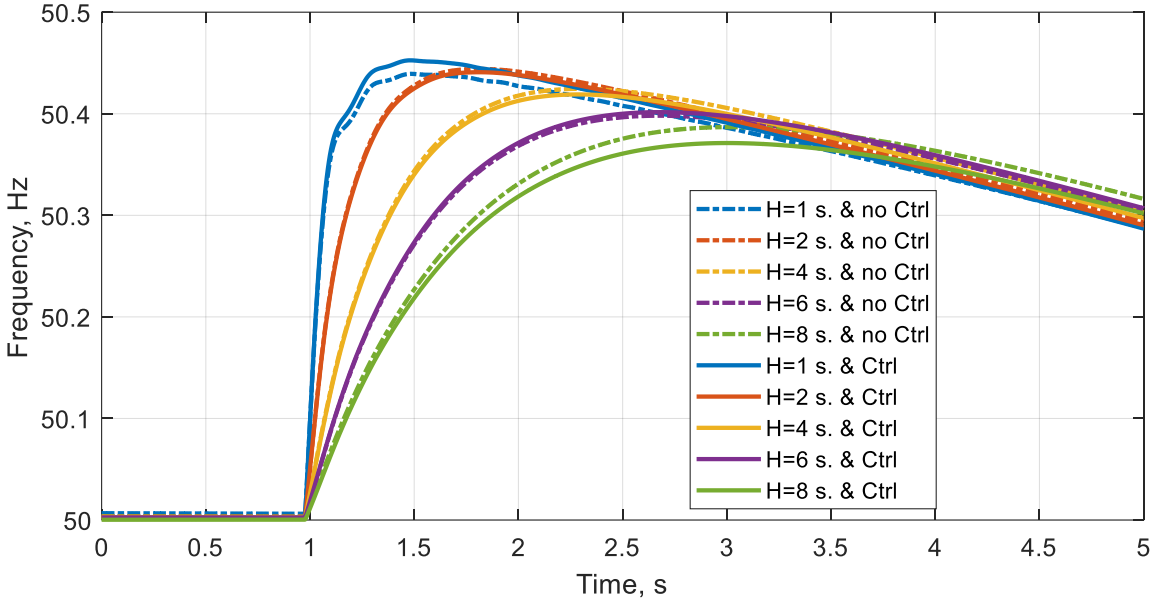


Fig. 4.12 Frequency dynamics of Area 1 with load reaction time of 500 ms.

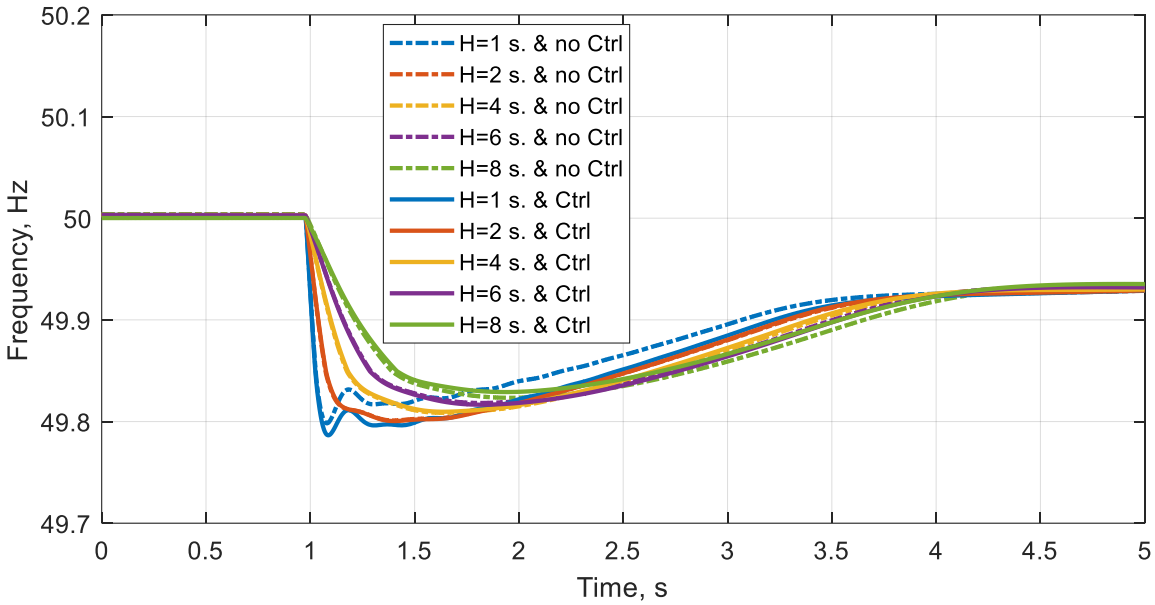


Fig. 4.13 Frequency dynamics of Area 2 with load reaction time of 500 ms.

From the previous tests and the results achieved, it can be inferred in general that the delay that was considered does not introduce significant changes in the dynamics of the system. The major impact can be observed mainly in the low inertia case. This is due to the natural response of the load to changes during frequency and voltage variations in the network, which leads to a positive effect for the system. In the particular tests, constant impedance load was used, which has quadratic dependence on voltage. This effect will have significant changes in the future due to the decarbonisation of the system and integration of more converter-interfaced generation (CIG) and electronic-driven loads, changing the nature of the system from constant impedance load to constant current/power loads, which should be considered in subsequent research.

### 4.2.3 Test with Initial Dynamic Model of Continental Europe

To test the concept of determination of grid separation and act more plausibly against its spreading, IDMCE was migrated to Opal-RT ePHASORSIM environment and executed in real time [17]. Model was extended with splitting cases such as the ones illustrated in Fig. 4.14 and Fig. 4.15.

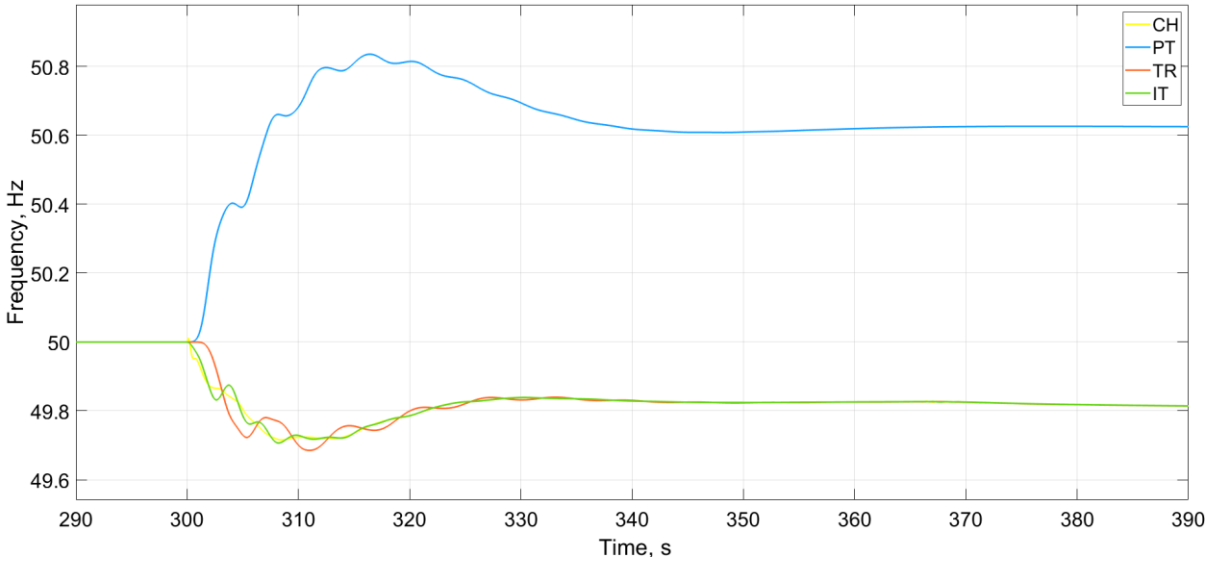


Fig. 4.14 Frequency dynamics under disconnection of FR, ES, and PT in real time environment.

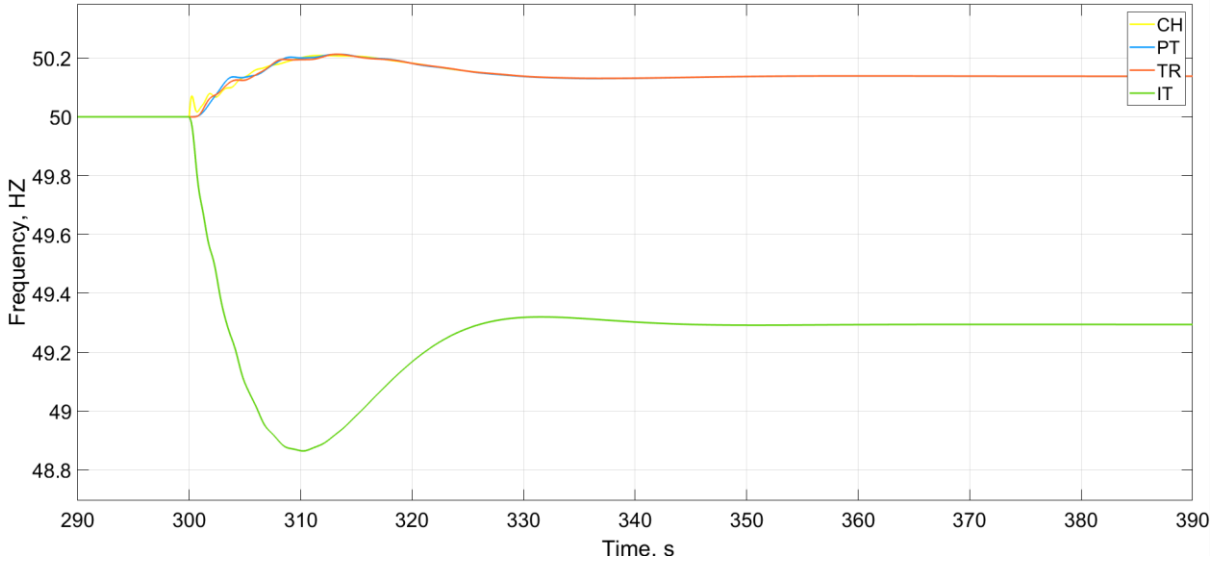


Fig. 4.15 Frequency dynamics under disconnection of IT in real time environment.

Then, several tests were carried out under controlled load cases and considering different aggregated asset poll sizes such as 0.1%, 0.5%, 1% and 2% out of 458 GW of total system load (equally distributed across IDMCE system with system inertia constant value variations). For a clearer effect, the thresholds for full activation of the pool were chosen in the range of 50 Hz +/- 150 mHz, and the frequency response under an illustration case involving the disconnection of Italy is show in Fig. 4.16.

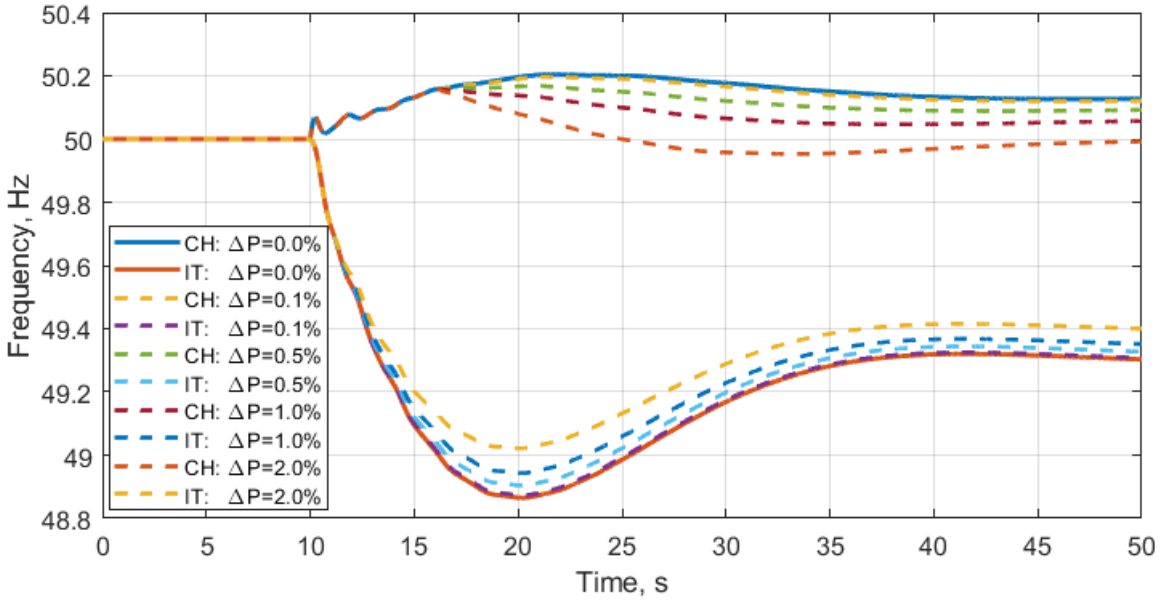


Fig. 4.16 Frequency dynamics under disconnection of IT in real time with different pool sizes.

Now, the results of the previous figure can be summarised as in Table IX and Fig. 4.17, where improvements in the frequency nadir/zenit for the case of load under control can be particularly observed.

Table IX. Frequency containment support to limit the nadir/zenith of the frequency.

| $\Delta P_{load}$ (%) | Over/Under production areas | Nadir/Zenith, Hz | | | |
|---|---|---|---|---|---|
| | | ΔH=0% | ΔH=-30% | ΔH=-50% | ΔH=-70% |
| 0% (base case) | Over | 50.204 | 50.220 | 50.234 | 50.252 |
| | Under | 48.865 | 48.796 | 48.739 | 48.674 |
| 0.1% | Over | 50.196 | 50.211 | 50.224 | 50.241 |
| | Under | 48.873 | 48.804 | 48.747 | 48.683 |
| 0.5% | Over | 50.168 | 50.179 | 50.188 | 50.199 |
| | Under | 48.904 | 48.837 | 48.782 | 48.719 |
| 1% | Over | 50.158 | 50.166 | 50.168 | 50.173 |
| | Under | 48.943 | 48.878 | 48.822 | 48.764 |
| 2% | Over | 50.158 | 50.166 | 50.168 | 50.173 |
| | Under | 49.022 | 48.962 | 48.912 | 48.855 |

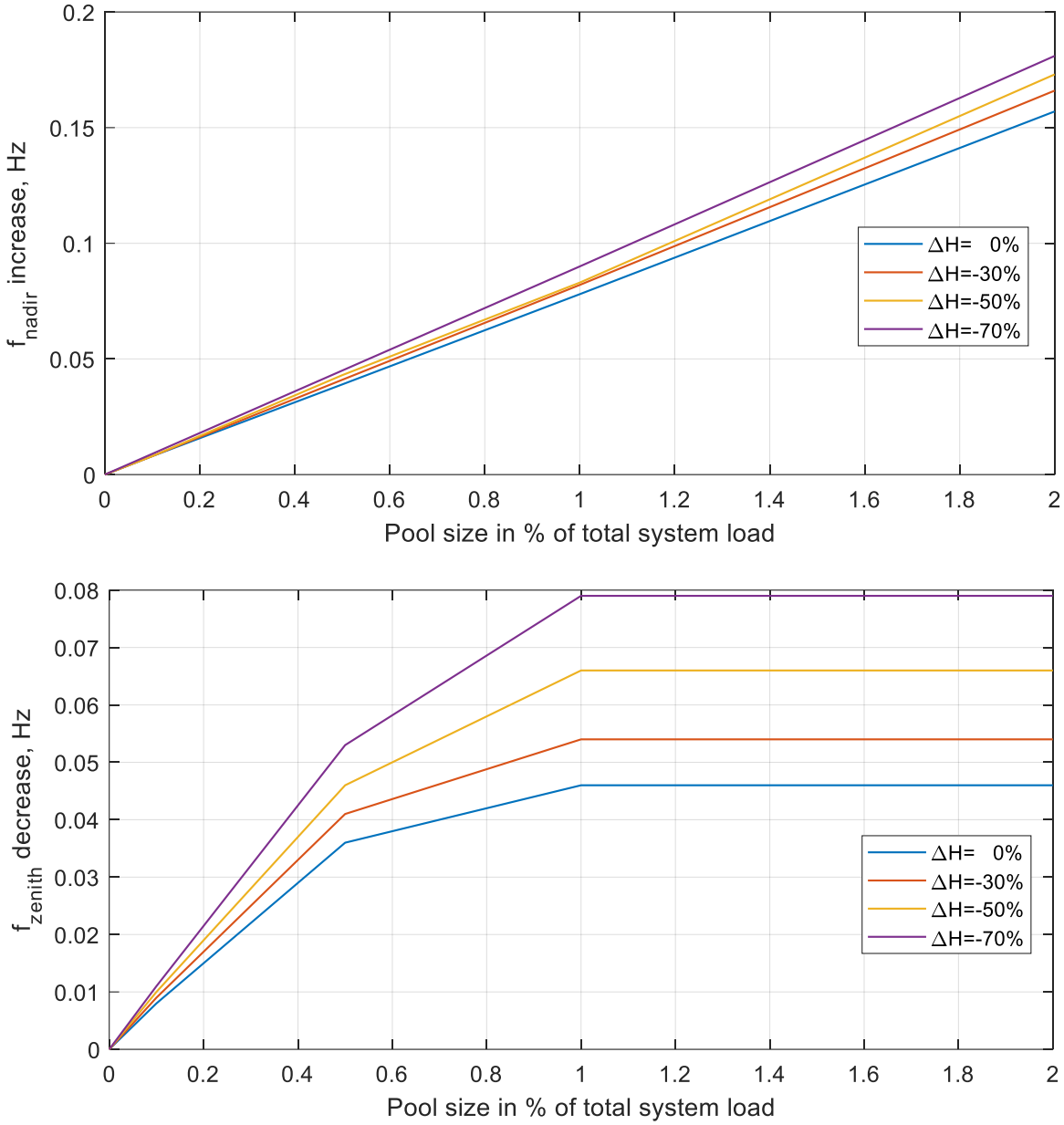


Fig. 4.17 Frequency containment support with decentralized scheme.

Achieved results show the positive effect and correct operation of decentralised devices within the entire power system and in cases of system split. The size of the pool's available load leads to frequency containment support to limit the frequency nadir/zenith, with a clear and great effect under reduced inertia scenarios. However, a negative effect was also detected for over-contribution situations – if the pool size is bigger than the necessary for containment of over frequency, a transient frequency drop below the nominal value could happen (as shown by the curve “CH: ΔP=2.0%” in figure 4.16) and potentially lead to frequency fluctuations. This effect was not considered in more detail within the framework of the project, but this issue remains open, and a more detailed study is necessary, as well as possible further improvement of a decentralised system with new settings and time delays.

# 5 Conclusions

An extensive number of simulations were performed to analyse and quantify the impact that a malfunction or non-intentional and undesired control of large OEM asset pools may have on the frequency stability of the Continental European Power System. Regarding interconnected operation, simulation results showed that tolerable RoCoF values can be achieved for different variations in system inertia even for relatively large power imbalances (such as 24 GW). However, any deficit of active power that exceeds the actual amount of FCR may endanger containment of frequency deviations and lead the operation of under-frequency load shedding (UFLS) protection. With the increasing proliferation of cloud aggregated assets, the potential incidence of more critical imbalances will raise and more FCRs can be required to adequately avoid frequency degradation. Unfortunately, an increment in power reserves also implies an important increase of related costs per year.

According to the simulation results from considered system split scenarios, RoCoFs superior to 1 Hz/s were noticed, including values greater than 2 Hz/s under particular split circumstances and overall inertia reductions. In practice, relatively high RoCoFs may result in uncontrolled cascading failures, and eventually the system collapse, due to mechanical limitations of synchronous machines and ineffective operation of UFLS schemes to arrest critical frequency declines (shorter time margin to react).

It is recognized that, although cloud solutions can provide different key benefits to power systems, cyber security aspects must be addressed to minimize the impact of any breach in this sense. Therefore, the evaluation of risks and the adoption of corresponding mitigation strategies need to be determined by a reliable cloud risk assessment model.

Due to the importance of limiting the impacts of system splits, two support methods were implemented (with industrial devices provided by tiko and a HIL setup) to limit the nadir/zenith of frequency through pools of assets. As for this, the main concerns of the centralised approach are the need for additional measuring infrastructure for frequency measurement, the selection of critical points in terms of power system separation, and a stable communication. These aspects greatly complicate the effectiveness of the method and introduce a greater number of changing and unpredictable events that do not guarantee system robustness. On the other hand, the decentralised method does not have these disadvantages and makes decisions locally based on continuously changing settings. However, this is also a disadvantage at the same time since the pool operator cannot unambiguously determine where and at what settings the on/off switching will occur. Through internal discussions, lab-scale setup, and results analysis, a decentralised method was chosen as the preferred one, with further integration in the pool. From the large power system tests, this method proved itself to work in the case of thousands of small loads under control and provide frequency support in the event of a system split. The proposed decentralised frequency method of aggregated pool represents a limited frequency sensitive mode (LFSM Under- and Over-Frequency), defined by ENTSO-E network codes on grid connection, to maintain the stability of the power system in emergency situations. Then, when the frequency overpasses 50.2 Hz, the aggregator pool can quickly increase its active power injection according to a pre-defined droop. On the other side, when the frequency drops below 49.8 Hz, pool loads can quickly decrease their active power consumption according to a pre-defined droop. Therefore, future large OEM asset pools need to consider LFSMs in their pools according to the TSO's requirements.

# 6 Outlook and next steps

As the platform of tiko is designed for virtual power plant functionalities at Ancillary Services and Energy Markets, the results of the IMPALA project gave tiko an overview and outlook about where the company can profit better and deliver the indicated services in robust and optimized manner. Therefore, tiko AG will exploit the results of the project within its future business model and market, considering for example the more than 30,000 controllable heating devices in France.

Besides, from a research perspective, ZHAW will use the results of the project in further studies related to the following topics:

- The substantial deployment of non-synchronous energy resources and displacement of synchronous generators (SGs) is affecting the capability of the grid to effectively counteract and control the effects of sudden power imbalances. With the establishment of new business models based on cloud aggregate assets and the expansion of ICTs, the problem becomes even more complex due the possibility to lose a large pool of assets operating under this scheme and the drastic RoCoFs and frequency deviations it may lead to. Then, the reliable and secure operation of the system under such emerging scenarios calls for the development of innovative solutions that can detect critical stability conditions early on and deploy timely preventive/corrective actions to avoid a potential system collapse.

- Since the more inertia the system has the better its capability to resist dynamic changes, the continuous monitoring and quantification of available inertia under significant shares of CIG becomes also of paramount importance. Therefore, reliable methods and instruments to efficiently and accurately achieve this task in real time need to be developed and implemented. In this way, required supporting means could be opportunely applied before system inertia falls below a given critical value.

- With the negative alteration of the natural and instantaneous response to frequency disturbances when the number of online SGs is reduced, new sources and mechanism that can somehow replicate this inherent dynamic behaviour of SGs have to be implemented. Although CIG with grid-forming control can be exploited to mimic physical inertial response, there are many technical issues to be clarified before such solution can be widely adopted in practice. In this sense, grid-forming inverter concerns regarding for example system stability, seamless transfer between stand-alone and grid connected mode, as well as fault ride through and overcurrent protection, demand further investigation.

- Now, although the cybersecurity events in this project were basically simulated in terms of the direct disconnection/reconnection of a massive set of predefined components, randomly accommodated across the whole test system, an improved and more advanced approach where the communication network dynamics are also modelled and incorporated into the environment of analysis can be followed for a more realistic approach.

Achieved results have also provided to Swissgrid an overview of the system split consequences in the region, in order to properly consider necessary requirements on a daily basis to potentisally mitigate the risks of occurrence.

Finally, RISE will use gathered results and scripts from the project for further investigation of the Nordic Power system considering system splits and potentially new special protection schemes.

# 7 National and international cooperation

The activities presented in this report have been achieved in close collaboration with the partners of the consortium (Tiko AG, Swissgrid, and the Swedish Research Institute RISE under ISGAN WG 5 and 6). All of them have supported the development of project activities by following up, participating in meetings, providing feedback, and contributing with their technical experience.

# 8 Publications and dissemination

- W. Sattinger, M. Ramirez, E. Hillberg, R. Segundo, A. Obusevs, A. Chacko, D. Clauss, P. Korba, “Impact of aggregated assets in the power system,” CIGRE Session, Paris, France, Aug. 2022.
- A. Obushevs, M. Ramirez-Gonzalez, P. Korba “IMPALA: Impact of aggregated electrical assets on the electrical power system” IEA_ISGAN WG 5 SIRFN- Knowledge-Sharing, Dec. 2023

# 9 References

[1] Solar Power Europe, “EU solar boom: over 100% solar market increase in 2019.” https://www.solarpowereurope.org/eu-solar-boom-over-100-solar-market-increase-in-2019/.
[2] ENTSO-E Report, “Frequency Stability Evaluation Criteria for the Synchronous Zone of Continental Europe: Requirements and impacting factors,” RG-CE System Protection & Dynamics Sub Group, March 2016.
[3] InsideEVs, “Plug-In Car Registrations in Europe: Q1-Q2 2021 Full Report,” https://insideevs.com/news/527912/plugin-car-registrations-europe-2021q1q2/ (accessed August 27, 2021).
[4] Statista, “Total number of battery electric cars registered in Germany from 2008 to 2021,” https://www.statista.com/statistics/646075/total-number-electric-cars-germany/ (accessed August 27, 2021).
[5] U. Cali, M. Kuzlu, M. Pipattanasomporn, J. Kempf, L. Bai, “Digitalization of Power Markets and Systems Using Energy Informatics”, Cham: Springer, 2021.
[6] S. Zhang, A. Pandey, X. Luo, M. Powell, R. Banerji, L. Fang, A. Parchure, E. Luzcando, “Practical Adoption of Cloud Computing in Power Systems—Drivers, Challenges, Guidance, and Real-World Use Cases,” IEEE Transactions on Smart Grid, vol. 13 (3), pp. 2390-2411, 2022.
[7] H. H. Alhelou, N. Hatziargyriou, Z. Y. Dong, “Power Systems Cibersecurity: Methods, Concepts, and Best Practices”, Cham: Springer, 2023.
[8] Semerow, A., Höhn, S., Luther, M., et al.: “Dynamic Study Model for the Interconnected Power System of Continental Europe in Different Simulation Tools,” IEEE PowerTech, Eindhoven, Netherlands, July 2015, pp. 1–6.
[9] UCTE Report, “28 September 2003 Blackout in Italy,” April/2004.
[10] UCTE Report, “System Disturbance on 4 November 2006,” /2007.
[11] ENTSO-E Report, “Separation of the Continental Europe power system on 8 January 2021,” July/2021.
[12] ENTSO-E Report, “Continental Europe Synchronous Area Separation on 24 July 2021,” July/2021.
[13] ENTSO-E Report, “Inertia and Rate of Change of Frequency (RoCoF),” SPD – Inertia TF, 16/Dec/2020.
[14] ENTSO-E Report, “Project Inertia – Phase II: Updated frequency stability analysis in long term scenarios, relevant solutions and mitigation measures,” November/2023.
[15] ZHAW REE-lab description: https://infrastructure.der-lab.net/zurich-university-of-applied-sciences-zhaw/
[16] P. Kundur, Neal J. Balu, and Mark G. Lauby, “Power system stability and control”, vol. 7. New York: McGraw-hill, 1994.
[17] A.Obusevs, “Real-Time Transient Stability Simulation of ENTSO-E Initial Dynamic Model of Continental Europe”, OPAL-RT’s Conference on Real-Time Simulation, 2019.